Geophysical Journal International

Geophys. J. Int. (2013) **194,** 1374–1389
Advance Access publication 2013 July 12

doi: 10.1093/gji/ggt181

Magnetic inclination shallowing problem and the issue of Eurasia's rigidity: insights following a palaeomagnetic study of upper Cretaceous basalts and redbeds from SE China

Yong-Xiang Li,[1] Liangshu Shu,[1] Bin Wen,[1] Zhenyu Yang[1] and Jason R. Ali[2]

[1]*State Key Laboratory for Mineral Deposits Research (Nanjing University), School of Earth Sciences and Engineering, Nanjing University, Nanjing* 210093*, China. E-mail: yxli@nju.edu.cn*
[2]*Department of Earth Sciences, The University of Hong Kong, Pokfulam Road, Hong Kong SAR, China*

Accepted 2013 May 4. Received 2013 April 27; in original form 2012 December 6

SUMMARY

Redbeds are an important source of palaeomagnetic data, but they often record inclinations shallower than that of the ancient local geomagnetic field. Discrepancy of palaeopoles from Cretaceous redbeds in South China Block (SCB) and the coeval Eurasia reference pole is commonly attributed to inclination shallowing. However, redbed-derived palaeomagnetic data from the block have rarely been critically assessed with data from coeval volcanic rocks that should be unaffected by the problem. Here, we address the issue using high-quality palaeomagnetic data from Upper Cretaceous (∼95 Ma) amygdaloidal basalts and coeval redbeds from Jiangshan, Zhejiang Province and Guangfeng, Jiangxi Province. Stepwise thermal and alternating field demagnetizations isolated stable components that in the basalts are carried by a mixture of magnetite and titanomagntite and in the sedimentary units by haematite. The stable components are regarded as primary based on positive intraformational conglomerate tests and a regional tilt test. The redbeds yield a tilt corrected mean direction of $D = 20.9^\circ$, $I = 35.8^\circ$, $\alpha_{95} = 8.7^\circ$, $N = 6$, which is statistically indistinguishable from the mean direction of the basalts ($D = 17.6^\circ$, $I = 38.1^\circ$, $\alpha_{95} = 8.6^\circ$, $N = 11$), suggesting that the former do not suffer from the problem. In addition, analysis of the other Late Cretaceous SCB palaeopoles reveals two groups with one at relatively high ('H', ∼80°N) latitudes and the other at relatively low ('L', ∼70°N) latitudes. Importantly, each comprises palaeopoles from both redbeds and volcanic rocks, and reasonable consistency exists within each group, further attesting that SCB redbeds do not suffer significant inclination shallowing. Comparison of the SCB palaeopoles with a newly defined coeval reference pole for Europe indicates an ∼11° separation. Since inclination shallowing, over 1000 km tectonic shortening, and apparent polar wander appear unlikely, the ∼11° discrepancy may provide evidence for the non-rigidity of the Eurasia plate. Consequently, a new Late Cretaceous reference pole for the stable SCB is defined at 72.3°N, 235.2°E, where $A_{95} = 3.2^\circ$ and $N = 6$.

Key words: Palaeomagnetism applied to tectonics; Palaeomagnetism applied to geologic processes; Rock and mineral magnetism.

1 INTRODUCTION

Continental redbeds are frequently used in palaeomagnetic studies because of their widespread occurrence and their ability to carry stable remanences. Additionally, they often average out secular variation, which is sometimes a problem with igneous rocks. However, redbeds frequently record shallower-than-expected inclinations (Tauxe & Kent 1984; Gareces *et al.* 1996; Gilder *et al.* 2001; Tan *et al.* 2003, 2010; Bilardello & Kodama 2010). This enigmatic phenomenon is perhaps best exemplified in Central Asia where the anomalously shallow inclinations from various Cretaceous formations have sparked a heated debate as to their origin. Explanations include tectonic shortening (e.g. Chen *et al.* 1992), non-dipole geomagnetic fields (e.g. Si & Van der Voo 2001), intracontinental deformation (e.g. Cogné *et al.* 1999), and inclination shallowing or recording errors of redbeds (e.g. Gilder *et al.* 2003; Tan *et al.* 2003, 2010).

In South China, most of the palaeomagnetic data for late Mesozoic units are from redbeds (see compilation of Sato *et al.* 2011). However, in recent years, concerns have been increasingly raised about whether the data set is contaminated with results that have experienced inclination shallowing (e.g. Narumoto *et al.* 2006; Sun *et al.* 2006; Wang & Yang 2007; Otofuji *et al.* 2010; Sato *et al.* 2011). Previous studies have consistently shown that the South China Block

(SCB) had arrived at its basic current position by the Early Cretaceous (e.g. Enkin *et al.* 1992). Since then it has been considered as a coherent part of eastern Asia (Tapponnier *et al*. 1982; Liu & Morinaga 1999; Morinaga & Liu 2004; Tsuneki *et al.* 2009) except for its fault-bounded southwestern and southeastern margins that experienced local and/or regional deformation and microblock rotations associated with the India–Asia collision and subduction of the Pacific plate beneath Asia (e.g. Funahara *et al.* 1992; Gilder *et al.* 1993; Otofuji *et al.* 1998; Yoshioka *et al.* 2003; Ali *et al.* 2004; Tamai *et al.* 2004; Li *et al.* 2005). However, recent studies of redbeds from the central SCB have reported anomalously low inclinations (Narumoto *et al.* 2006; Sun *et al.* 2006; Wang & Yang 2007). Such behaviour suggests that redbeds in South China do not faithfully record the geomagnetic field, or that the SCB underwent latitudinal displacement relative to Europe since the Late Cretaceous, contradicting the long-held view of a rigid Eurasia plate. An independent means of establishing whether redbeds suffered inclination shallowing involves investigating the palaeomagnetism of coeval volcanic rocks and to compare the directions of the two lithotypes; the latter are ostensibly immune from the problem, though not always providing complete averaging of secular variations. However, few studies have examined the palaeomagnetism of the Late Cretaceous volcanic rocks in the SCB, partly because coeval volcanic rocks are relatively rare. In this study, we carried out a palaeomagnetic investigation of Upper Cretaceous basalts from the central SCB. Notably, the studied basalts are either intercalated with redbeds or contain distinct, flattened vesicles and amygdales, which allows the palaeohorizontal to be readily deduced. We also sampled the associated redbeds to compare the directions of these two lithotypes to examine whether redbeds in the SCB suffered inclination shallowing. This study not only provides a robust test for the accuracy of magnetic inclination of redbeds in the SCB, but also provides a means of evaluating whether the Eurasia plate experienced intracontinental deformation.

2 GEOLOGICAL SETTING

The SCB comprises the Yangtze Block to the northwest and Cathaysia Block to the southeast. They are separated by the Jiangshan–Shaoxin–Pingxiang fault zone (Fig. 1) (e.g. Charvet *et al.* 1996; Gilder *et al.* 1996). It is widely accepted that the two sutured in the early Neoproterozic (Guo *et al.* 1989; Shu *et al.* 1994; Shu & Charvet 1996; Wang *et al.* 2007; Li *et al.* 2009; Charvet *et al.* 2010; Shu *et al.* 2011). The SCB is believed to have rifted from northeastern Gondwana in the Devonian drifting northwards across the eastern Tethys (Metcalfe 1996). It amalgamated with the North China Block (NCB) between mid-Permian and the Late Triassic (Enkin *et al.* 1992; Metcalfe 1996, 2002; Li 1998). During the Late Triassic to the Early Jurassic, a convergent margin developed on the southeast side of the SCB. Subduction of palaeo-Pacific plate produced widespread magmatism (Lapierre *et al.* 1997; Charvet *et al.* 1999; Li 2000; Zhou *et al.* 2006). Additionally, a major northeast-trending fold and thrust belt developed spanning the Late Triassic to the Early Jurassic (Li & Li 2007). During the Middle Jurassic–Late Cretaceous, regional-scale extension occurred in

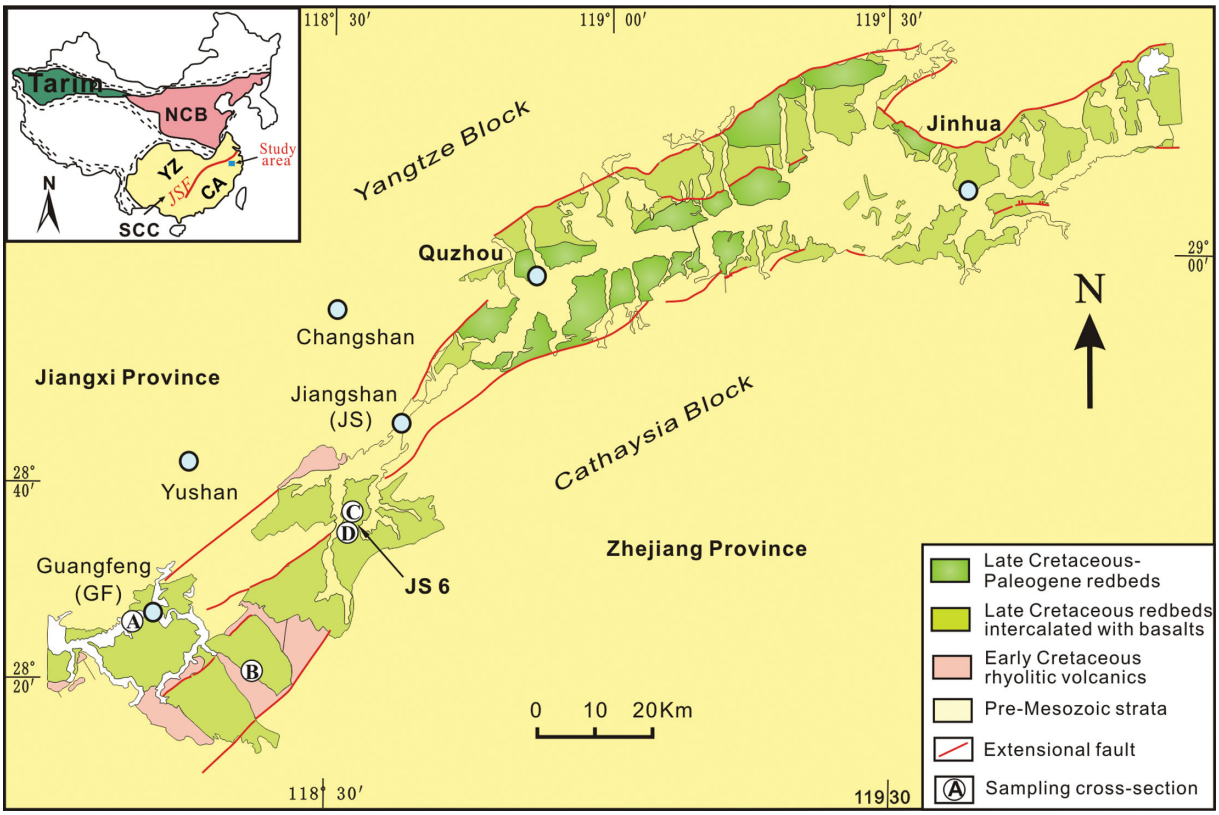

Figure 1. Simplified geological map showing the study area, sampling localities and the representative stratigraphic columns. The study area is located in the northeastern part of the SCB. The SCB comprises the Yangtze (YZ) craton to the northwest and the Cathaysia (CA) block to the southeast, separated by the Jiangshan–Shaoxin fault (JSF); samples were collected from Jiangshan (JS), Zhejiang Province and Guangfeng (GF), Jiangxi Province. Both areas are geologically situated within the NE-striking basin which is filled with kilometre-thick Upper Cretaceous redbeds and intercalated basalts. Samples were collected from the upper Cretaceous Zhongdai Formation (K2z) and the studied rocks are estimated to be at 90–100 Ma. NCB, North China Block.

southeast China as a result of the Pacific Plate subduction (Xu *et al.* 1987; Gilder *et al.* 1991; Li 2000; Ren *et al.* 2002; Shu *et al.* 2009). This gave rise to numerous peraluminous granitic plutons, various magmatic assemblages indicative of extension and numerous NE-striking volcanic-sedimentary basins (Ren *et al.* 2002; Shu *et al.* 2009). The latter were filled with thick piles of continental sediments and occasional alkaline basalts (Cai & Yu 2001; Yu *et al.* 2004; Wang & Shu 2012). The extensional tectonism in the southeastern China was punctuated by a brief episode of uplift at 100 Ma, which was probably due to the influence of an oblique-collision between Japan–Taiwan Arc and palaeo-Pacific plate (Ichikawa *et al.* 1990; Lo & Yui 1996).

3 SAMPLING

Samples were collected from the northeasterly elongated Xinjiang–Jingqu basins that straddle the boundary of Jiangxi and Zhejiang provinces (Fig. 1). The main rock types preserved in the basin comprise purplish-red or brick-red mudstones, siltstones, fine to coarse-grained sandstones and conglomerates (Cai & Yu 2001; Wang *et al.* 2002a). Volcanic rocks sporadically occur as interbeds within the lower part of the sequence increasing in abundance towards the coast of Zhejiang Province (Lapierre *et al.* 1997; Yu *et al.* 2001). The redbeds in the study area belong to the Upper Cretaceous Qujiang Group (K2qz). They can be divided into, from the bottom to the top, the Zhongdai (K2z), Jinhua (K2j) and Quxian (K2q) Formations (Bureau of Geology and Mineral Resources of Zhejiang Province 1996). Our samples were collected from the Zhongdai Formation (K2z). Radiometric dating of interbedded volcanic rocks and the presence of fossils such as vertebrates, plants, ostracods, gastropods, and dinosaur eggs in the equivalent redbeds in neighboring basins suggest that the studied rocks were formed in the early Late Cretaceous (Bureau of Geology and Mineral Resources of Zhejiang Province 1996; Cai & Yu 2001; Wang *et al.* 2002b; Yu *et al.* 2004; Shu *et al.* 2009; Wang & Shu 2012). The Ar/K ages of basalts within the basin range from ∼101.8 Ma (Li *et al.* 1989) to ∼91.7 Ma (Wang *et al.* 2002b). Cretaceous volcanic rocks have different geochemical signatures from those of the Cenozoic (Cui *et al.* 2011). Recent dating of the Cretaceous volcanic rocks using the more precise Ar/Ar method shows that the ages span ∼126 to ∼88 Ma (Wang *et al.* 2010). Comparing the sampled Zhongdai Fm with the Ar/Ar-dated sections suggests that the sampled rocks are younger than ∼104 Ma and older than ∼88 Ma.

Samples were collected from Guangfeng in Jiangxi Province and Jiangshan in Zhejiang Province (Fig. 1). In the former, basalt samples were collected from a section (Fig. 2a) near Guanfeng Town and a roadcut (Fig. 2b) ∼20 km to the southeast. The volcanics near Guanfeng Town contain abundant calcite- and chlorite-filled amygdales that are generally flattened, aligned parallel or subparallel to each other, and collectively exhibit a 'preferred orientation' that is inclined towards the NW (∼310°) at ∼20°, which is consistent with the attitude of sedimentary interbeds. Thus, they almost certainly represent the palaeohorizontal at the time when lavas solidified. Another noteworthy feature is that the amygdales gradually decrease upward in size, typically at centimetre scale at bases of flows, reducing upward to millimeters before in some cases disappearing. An interval containing vesicles and amygdales of a complete grade of sizes is considered to represent a single lava-flow event. Based on this feature, we recognized three such units in the ∼100 m thick section of the amygdaloidal basalts near Guangfeng Town. Furthermore, within the uppermost flow is a probably contemporaneous diabase dyke. Four sites were collected from this section, one from each basalt flow and the other from the dykes.

The roadcut section in Guangfeng area (Fig. 2b) comprises at least five basalt flows that are overlain by red siltsones/sandstones interbedded with reddish shales. The five basalt flows were distinguished based on the difference in textures such as the absence/presence/abundance/rareness of vesicles and amygdales, and lava breccias. The thickness of each flow ranges from a few metres to up to 200 m. Four sites, one per flow, were collected. In addition, three sites were sampled from the overlying redbeds. The vesicles/amygdales in the basalts of this section are generally not as abundant as those in the Guangfeng Town section and do not exhibit distinct preferred orientations. Thus, the attitudes of the overlying redbeds were used as the bedding correction. Together with samples taken from the section near Guanfeng Town, we collected 11 sites in total from Guangfeng area including eight sites from basaltic units and three sites from red siltstones/sandstones.

In Jiangshan, Zhejiang Province, samples were collected from two outcrops in Chentangwu village and one in Guanghui village. The Chentangwu exposure consists of three amygdaloidal basalts that are intercalated with three red siltstone beds (Fig. 2c). Two redbeds are 1.0–1.5 m thick, while a third is about 20 cm thick. Two basaltic units are about 1 m thick, whereas a third basalt flow is massive, >20 m thick. At the base of the ∼1 m thick basalt bed, there are a few red siltstone lenses with tails linked to the underlying redbed, suggesting that these red lenses were entrained from the underlying redbed at the time of the eruptions. The massive basalt unit contains abundant vesicles and amygdales that are flattened and consistently aligned. The orientation of these vesicles and amygdales is subparallel to the bedding of the underlying redbeds, and can thus be used to determine the palaeohorizontal. Samples were collected from two basalt flows and each of the red siltstone beds. Red lenses at the base of the ∼1 m thick basal bed were also sampled to perform a conglomerate test (site JS3). About 200 m southwest to the Chentangwu section is a quarry (Fig. 2d) where we collected one basalt flow site. In the neighbouring Guanghui village, which is about 3 km to the southwest, a basaltic agglomorate bed is well exposed (Fig. 1, JS6). Both the matrix and the rounded clasts of the conglomerate are basalts in composition, and thus the basaltic conglomerate bed likely occurs within a massive basalt unit as seen in the Chentangwu village section. We drilled 14 individual basaltic pebbles to conduct a conglomerate test (site JS6). Therefore, we collected eight sites in total from the Jiangshan area including three basalt flows, three redbeds and one red lens plus one site from the basaltic conglomerates.

Samples were collected with a gasoline-powered portable rock drill. Typically about ten 25 mm diameter cores were drilled at each site and each individual core was oriented with a magnetic compass mounted on an aluminum orientation device. Present-day declinations in Guangfeng and Jiangshan are −4.2 and −4.3, respectively, according to International Geomagnetic Reference Field (IGRF; Finlay *et al.* 2010), and thus −4 was used as the declination correction.

4 METHODS

In the laboratory, cores were trimmed to 2.2-cm-long standard palaeomagnetic cylindrical specimens using a dual-blade rock saw. Ten or more specimens are typically prepared for each site. Basalt specimens were subjected to either alternating field (AF) or

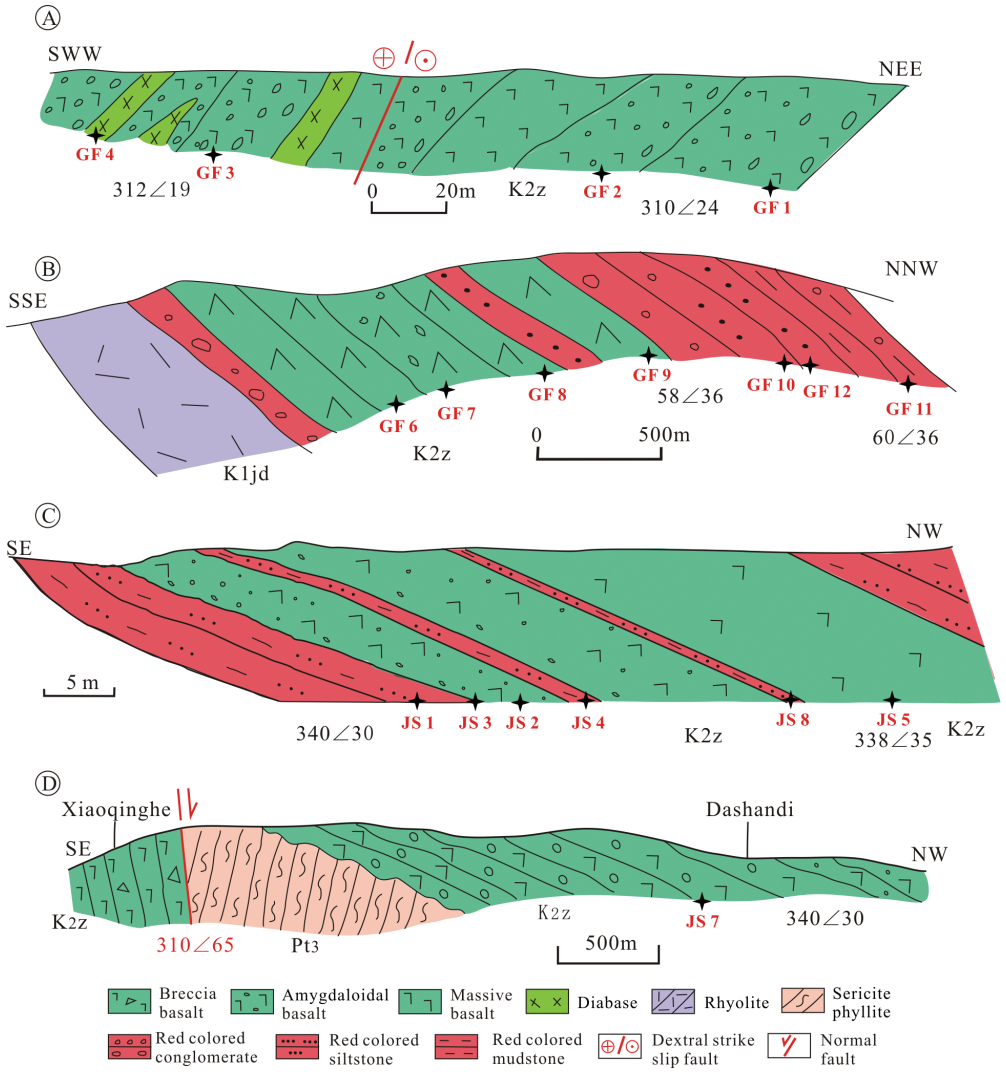

Figure 2. Schematic cross sections in Guangfeng (a, b) and Jiangshan (c, d) areas showing the basic structure and stratigraphic position of sampled rock units in each section. (a) The Southwestern Guangfeng Town; (b) roadcut about 20 km southeast to cross section A (Fig. 1); (c) Chentangwu; (d) Xiaoqinghe to Dashandi, which is located about 200 m southwest to cross section C; K1jd, the Lower Cretaceous Jiangde Group; K2z, Upper Cretaceous Zhongdai Formation; Crosses indicate sampling sites. The overall orientation of a road along which rocks are exposed is taken as the orientation of each section. The GPS coordinates and Strike/Dip data of each site are summarized in Table 1.

thermal demagnetization and all redbed specimens were thermally demagnetized. The progressive demagnetization was performed in increments up to 100 mT (on average, eight steps) for AF demagnetization and up to 680°C (typically 15 steps) for thermal demagnetization. The AF demagnetization was conducted using a Molspin demagnetizer and the thermal demagnetization was carried out with an ASC TD-48 Thermal Demagnetizer. Remanence of basalt specimens was measured with an AGICO JR6 spinner magnetometer and remanence measurements of redbeds were made with a 2G Enterprises Inc. (CA, USA) cryogenic magnetometer. Both rock magnetometers are housed in a magnetically-shielded room in the Nanjing University Paleomagnetism Laboratory.

The demagnetization data are visually presented with vector-endpoint diagrams (Zijderveld 1967). Remanence components were determined by means of principal component analysis (Kirschvink 1980) and site mean directions were analysed using Fisher statistics (Fisher 1953). Regional tilt tests with the direction-correction (DC) method (Enkin 2003) and conglomerate tests based on the statistics of Watson (1956) were used to constrain the timing of remanence acquisition. Palaeomagnetic software packages PMGSC (by Randolph Enkin) and PaleoMac (Cogné 2003) were used to perform data analyses and produce related figures.

Anisotropy of magnetic susceptibility (AMS) of representative basalt and redbed samples was measured with a Kappabridge KLY-3. Isothermal remanent magnetization (IRM) acquisition experiments were conducted with an ASC impulse magnetizer on 11 basalt specimens to aid the magnetic mineralogy determination. In each IRM acquisition run, a forward field was applied that gradually increased from 20 to 2400 mT in 11 incremental steps. Additionally, a Lowrie (1990) test was performed on four representative specimens to further delineate the magnetic mineralogy. The samples were magnetized in sequence along their Z, Y and X axes at fields of 2.4, 0.4 and 0.12 T, respectively. The composite IRM was then stepwise thermally demagnetized up to 680°C. High-temperature magnetic susceptibility was measured with a Kappabridge KLY-3 coupled with a CS-2 heating apparatus that has flow-through argon gas to avoid mineral alteration during heating.

5 RESULTS

5.1 Rock magnetic results

IRM acquisition curves of the basalt samples show that the majority of samples saturated ∼200 mT (Fig. 3a), suggesting that low-coercivity magnetic phases dominate. However, a few samples had much higher coercivities, not saturating until ∼2.0 T (Fig. 3a). Thermomagnetic properties show that magnetic susceptibility of basalt samples either drop gradually between 450 and 600°C (Figs 3b and d) or drop rapidly between 580 and 600°C (Fig. 3c), indicative of magnetite and titanomagnetite. The magnetic susceptibility of some basalt samples only reduced by 680°C (Fig. 3b), indicating the existence of haematite. The redbed samples show overall low magnetic susceptibilities and appear resistant to heating (Fig. 3e), indicating the dominance of haematite.

The Lowrie tests show that remanence of basalt samples mainly resides in the low-coercivity magnetic minerals (Figs 3f, g, h and i), likely magnetite and titanomagnetite. The AMS data of basalt samples show no preferred orientations in both geographic and stratigraphic coordinates (Figs 4a and b). The AMS data of redbed samples show no obvious fabrics in geographic coordinates and display oblate fabrics in stratigraphic coordinates with the minimum axes perpendicular to bedding and maximum axes parallel/subparallel to bedding. The anisotropy degree of the oblate fabrics is low and the average p value is only 1.05. Oblate fabrics are typical depositional origin and the presence of oblate fabrics suggests that the rocks may have not been deformed significantly by subsequent tectonism.

5.2 Palaeomagneic results

5.2.1 Guangfeng area

Natural remanent magnetization (NRM) intensities of the basalt samples vary from 0.2 to 3.6 A m^{-1} with the majority of values between 0.5 and 1.5 A m^{-1}. Both AF and thermal demagnetization successfully isolated characteristic remanent magnetizations (ChRMs). Most samples exhibit two-component magnetizations with the low-coercivity component being removed typically at 10–20 mT/200–300°C (Figs 5a–c). The high-coercivity component displays a trajectory decaying towards the origin (Figs 5a–c). The intensity of most demagnetized samples shows a rapid drop between 550 and 600°C (Figs 5b and c), suggesting that magnetite is the dominant remanence carrier. Some demagnetized samples show a gradual decrease in intensity between 450 and 600°C, suggesting the presence of titanomagnetite. In most cases, complete demagnetization was achieved at 600°C. However, in some cases, the samples still retained about 10 per cent of initial intensity at 600°C and complete demagnetization only occurred by 650–680°C, indicating the existence of haematite (Fig. 5c). These observations are consistent with the thermomagnetic measurements (Figs 3b and c) that show the diagnostic features of magnetite and titanomagnetite, and the presence of haematite. A DC tilt test (Enkin 2003) of site means of basalts from the two sections in Guangfeng area is positive with an optimum untilting at 82.5 ± 29.8 per cent, which is indistinguishable from the 100 per cent untilting (Figs 6a and b). Thus, the stable remanence components are regarded as primary TRMs acquired when basalts formed.

The NRM intensity of redbeds samples varies from ∼1.0×10^{-2} to 2.0×10^{-2} A m^{-1}. Demagnetization reveals two-component magnetizations (Fig. 5d) and the stable components were isolated after the weak components were removed at ∼300°C. The sharp drop of 30 per cent of the initial intensity from 650 to 680°C (Fig. 5d) suggests that haematite is the remanence carrier. Since the bedding attitudes of redbeds are generally consistent, it is not possible to perform a meaningful fold test for redbeds. Because the immediately underlying basalt sequences carry primary remanent magnetization, it is reasonable to believe that the redbeds also retain primary remanences.

5.2.2 Jiangshan area

The initial remanent magnetization intensities of basalts range from 0.5 to 5.0 A m^{-1}, mostly between 2.0 and 3.0 A m^{-1}. Most samples display single-component magnetizations after removal of a viscous component at 200°C/10 mT (Fig. 5e). About two-thirds of samples show a gradual decline in intensity from 450 to 600°C (Figs 5e–f), suggesting that titanomagnetite dominates the samples. Also, these samples often show a rapid drop in intensity at 100–150°C (Figs 5e–f), indicating that goethite likely resides in these samples. The remaining samples exhibit a sharp decrease in intensity between 550 and 600°C (Fig. 5g), indicative of magnetite. These samples retained about 10 per cent of intensity above 600°C that was completely removed at 650–680°C (Fig. 5g), indicating the presence of haematite in these samples. The dominance of titanomagnetite is also revealed by the thermomagnetic curves that are characterized by the gradual decline in magnetic susceptibility from ∼420–600°C (Fig. 3d). Basaltic pebbles at site JS6 yield ChRMs of widely distributed directions (Fig. 6c) and stability test of randomness results in $R_o = 4.72$, which is less than the critical value of $R_c = 5.98$ for $N = 14$ at 95 per cent confidence level, constituting a positive conglomerate test (Watson 1956).

The NRM intensity of redbeds in Jiangshan area ranges from 0.7 to ∼20×10^{-2} A m^{-1}. The demagnetization trajectories of redbed samples show that a weak component unblocks at 200°C and the rest of the demagnetization trajectory decays linearly towards the origin (Figs 5h and i), defining a single, stable ChRM. Unfortunately, the bedding attitudes of the redbeds show little variation; thus, it is not possible to perform a meaningful fold test for the ChRMs of the redbed samples from Jiangshan area. Four samples from the redbed clasts (site JS3), which occur at the base of the ∼1.0-m-thick basalt flow (Fig. 2) and were likely entrained from the underlying redbeds, yield widely scattered directions (Fig. 6d). These directions pass the randomness test at 95 per cent confidence level (Watson 1956), suggesting that the formation of basalt flow did not reset magnetizations of the underlying redbeds. Moreover, the positive conglomerate test of the intraformational conglomerate at site JS6 suggests that basalts in Jiangshan area carry primary TRMs. Thus, the ChRMs of redbeds in Jiangshan area are regarded as primary.

5.2.3 Mean directions of basalts and redbeds

Site mean data are summarized in Table 1. To compare palaeomagnetic directions from different types of lithology, site means of redbeds and basalts are grouped and computed to obtain the mean directions for redbeds and basalts, respectively. The site means of six redbed sites yield a tilt-corrected mean direction of Dec = 20.9°, Inc = 35.8°, with $k = 60.0$ and $\alpha_{95} = 8.7°$. The tilt-corrected mean direction of 11 basalt sites is Dec = 17.6°, Inc = 38.1°, with $k = 29.1$ and $\alpha_{95} = 8.6°$. Comparison of the two mean directions

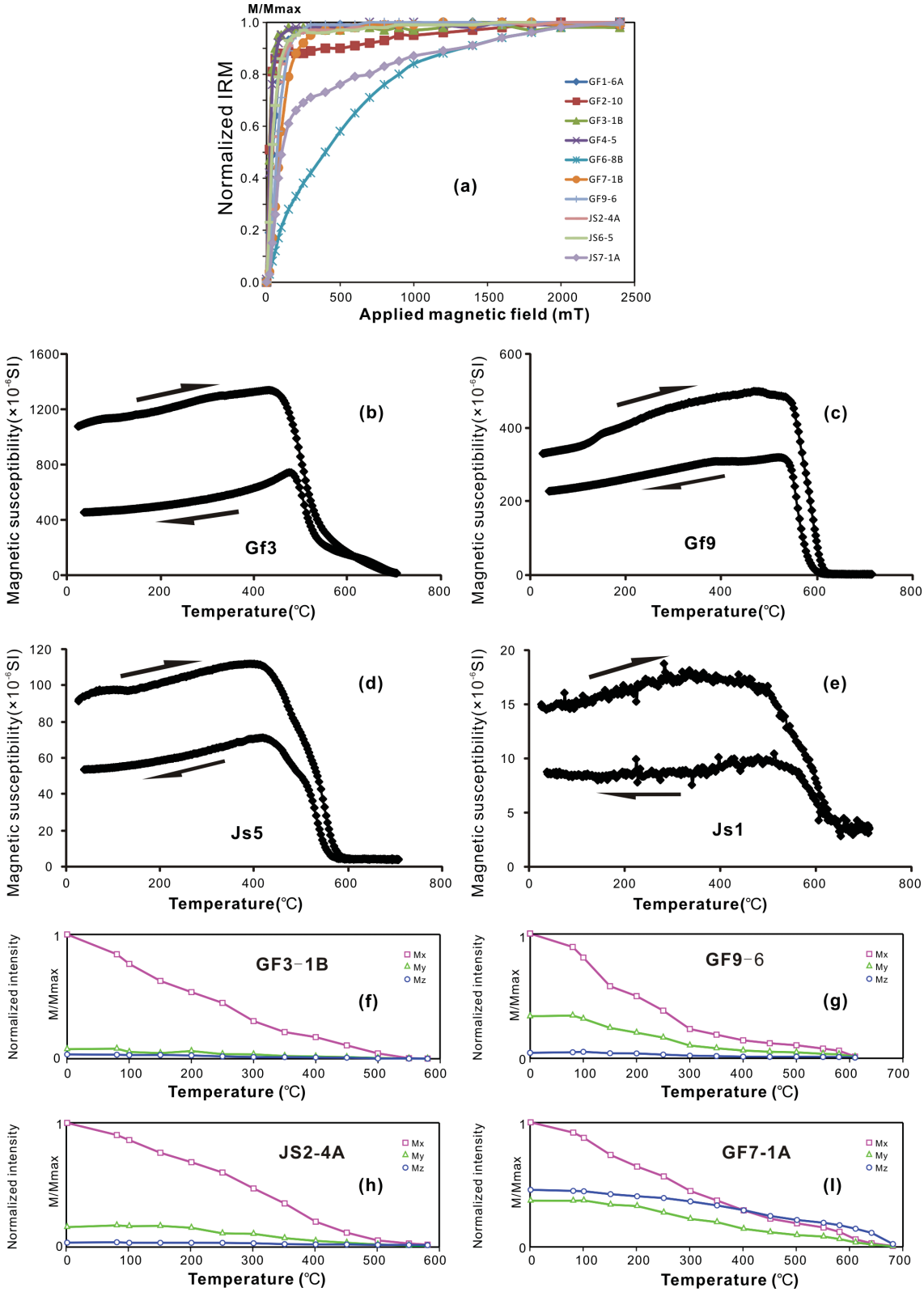

Figure 3. Rock magnetic results of the samples. (a) IRMs of representative basalt samples show that most samples are saturated by ~200 mT, suggesting the predominance of low coercivity phases in the basalt samples. (b)–(d) show thermomagnetic curves of representative basalt and redbeds samples. Basalts show either a rapid drop at ~580°C or a gradual decrease in susceptibility from ~450 to 600°C (b–d), suggesting that remanence resides in magnetite/titanomagnetite. Redbeds samples are relatively resistant to heating and show an overall weak susceptibility; the gentle decline in susceptibility from ~650 to 680°C (e) indicates that haematite is their major remanence carrier. (f)–(i) Lowrie tests of representative basalt samples show that remanence mainly resides in the low-coercivity phases.

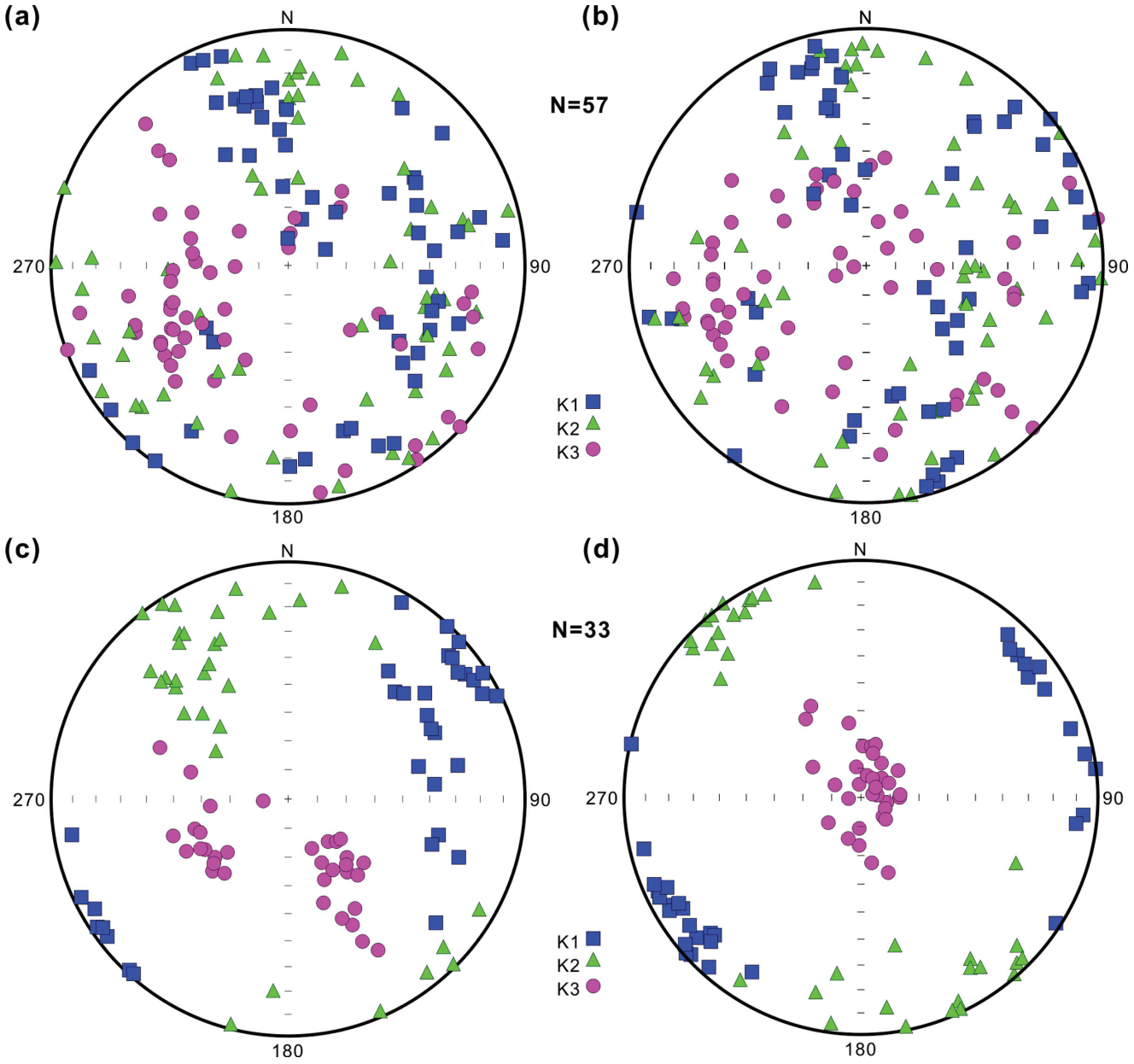

Figure 4. AMS data of the representative basalt (a, b) and redbed (c, d) samples in geographic (a, c) and stratigraphic (b, d) coordinates. The closed symbols are AMS principal axes in the lower hemisphere projections.

yields an angular separation of only 3.5°, which is well within the 95 per cent confidence limits of 8.7° and 8.6° for redbeds and basalts, respectively, indicating that the two mean directions are statistically indistinguishable.

The angular dispersion of virtual geomagnetic poles (VGPs) of the studied basalts is computed to be 16.4°, which is slightly greater than the predicted VGP scatter of ~ 8.0–13.0° for a palaeolatitude of 15–33° based on a palaeosecular variation model for 80–110 Ma (McFadden *et al*. 1991). But since the basalt sites represent 11 independent spot records of the geomagnetic field, the time span represented by the studied basalts should have averaged out the palaeosecular variation. The declinations of the site-mean directions are scattered (e.g. Fig. 6b), but the mean inclination is not changed. The mean of only inclinations is 36.4 ± 3.9°, which is similar to the inclination of 37.3 ± 6.0° of the Fisher mean. The spread in declinations of the site-mean directions likely resulted from the vertical-axis rotation of microblocks associated with the formation of the NE-striking basins in response to the extensional tectonism along the coastal SE China. Since the mean inclination is not changed, the main argument is not affected. In addition, the mean of the VGPs from basalts is 72.3°N, 226.2°E where $A_{95} = 9.5°$, $N = 11$ and is indistinguishable from the mean (69.0°N, 228.1°E, $A_{95} = 10.0°$, $N = 6$) of the VGPs from redbeds, demonstrating that palaeomagnetic results from basalts have averaged out secular variation. Therefore, the site means of basalts and redbeds are combined to compute a grand mean direction of the study area: Dec = 18.8°, Inc = 37.3°, k = 36.9 and α_{95} = 6.0°, N = 17 in stratigraphic coordinates. The mean of VGPs from both redbeds and basalts is located at 71.1°N, 226.9°E, $A_{95} = 6.6°$ and thus represents a ~95 Ma palaeopole for the SCB.

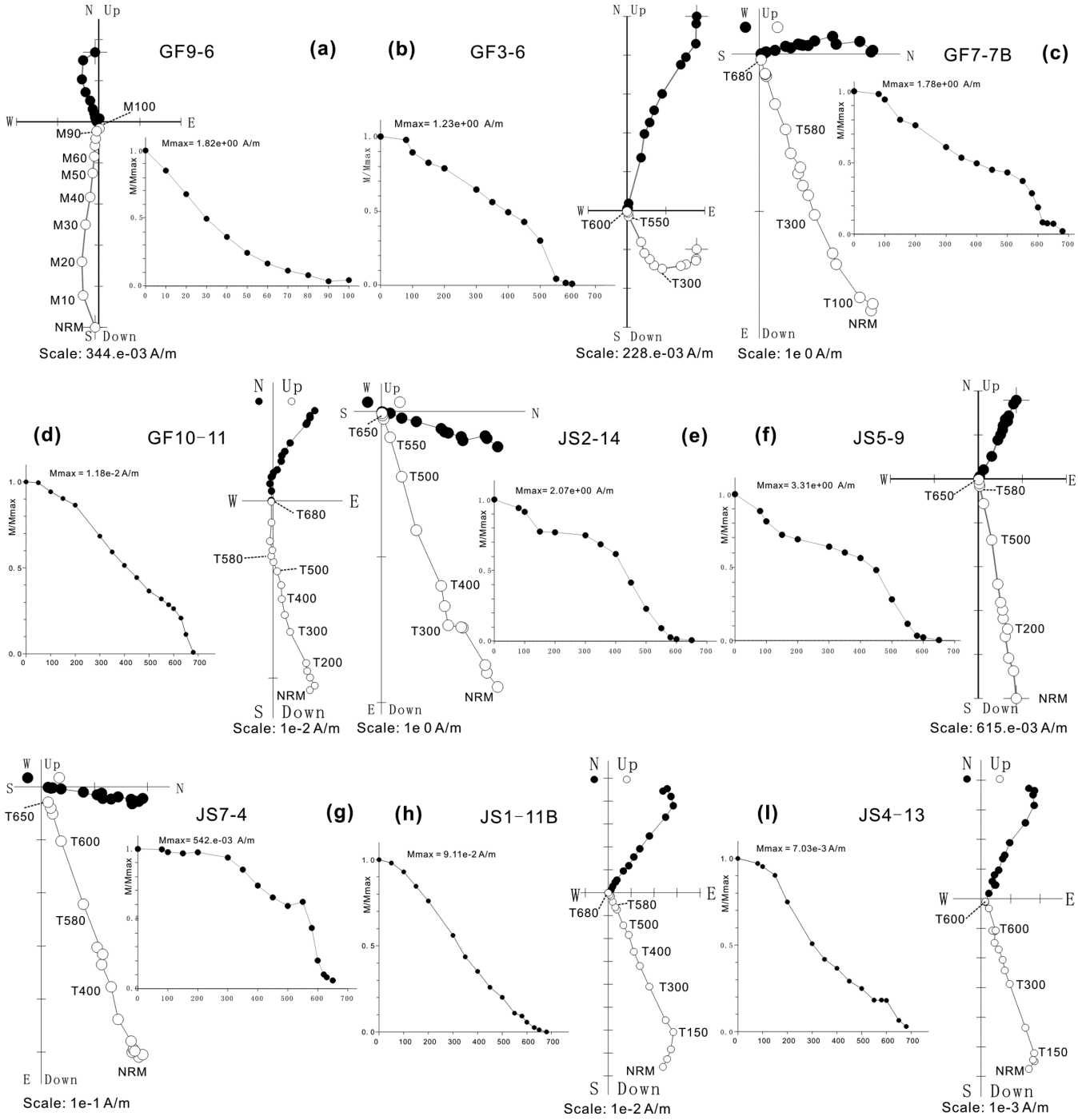

Figure 5. Representative vector-end plots (Zijderveld 1967) for AF (a–f) and thermal demagnetization of basalt (a–g) and redbed samples (h, i) in geographic coordinates. Solid squares indicate the horizontal components, and the open squares denote the vertical components.

6 DISCUSSION

6.1 Late Cretaceous palaeomagnetic poles from South China

The palaeopoles obtained in this study and other reliable Late Cretaceous poles (100–65 Ma) for South China are listed in Table 2. This table is mainly based on an earlier compilation (Li *et al.* 2005), which involved a rigorous quality evaluation ($Q = \geq 5$) based on the reliability criteria of van der Voo (1990) and includes several newer entries (Narumoto *et al.* 2006; Sun *et al.* 2006; Zhu *et al.* 2006; Wang & Yang 2007). The palaeopole from Jitai Basin, Jiangxi Province (Gu & Gu 1990), was previously assigned a Q value of 5 (Ma *et al.* 1993; Li *et al.* 2005), but no data and analytical details are available for critical examination because the results have so far only been reported as a symposium abstract. Thus, this pole is excluded. In addition, the Late Cretaceous palaeopoles from Zhejiang and Fujian provinces (Hu *et al.* 1990; Gilder *et al.* 1993; Liu *et al.* 1999) are superseded by the more recent, detailed results (Morinaga & Liu 2004).

Among the reliable palaeopoles, two palaeopoles, one from Jishui of Jiangxi (Wang & Yang 2007) and the other from north of Qinzhou

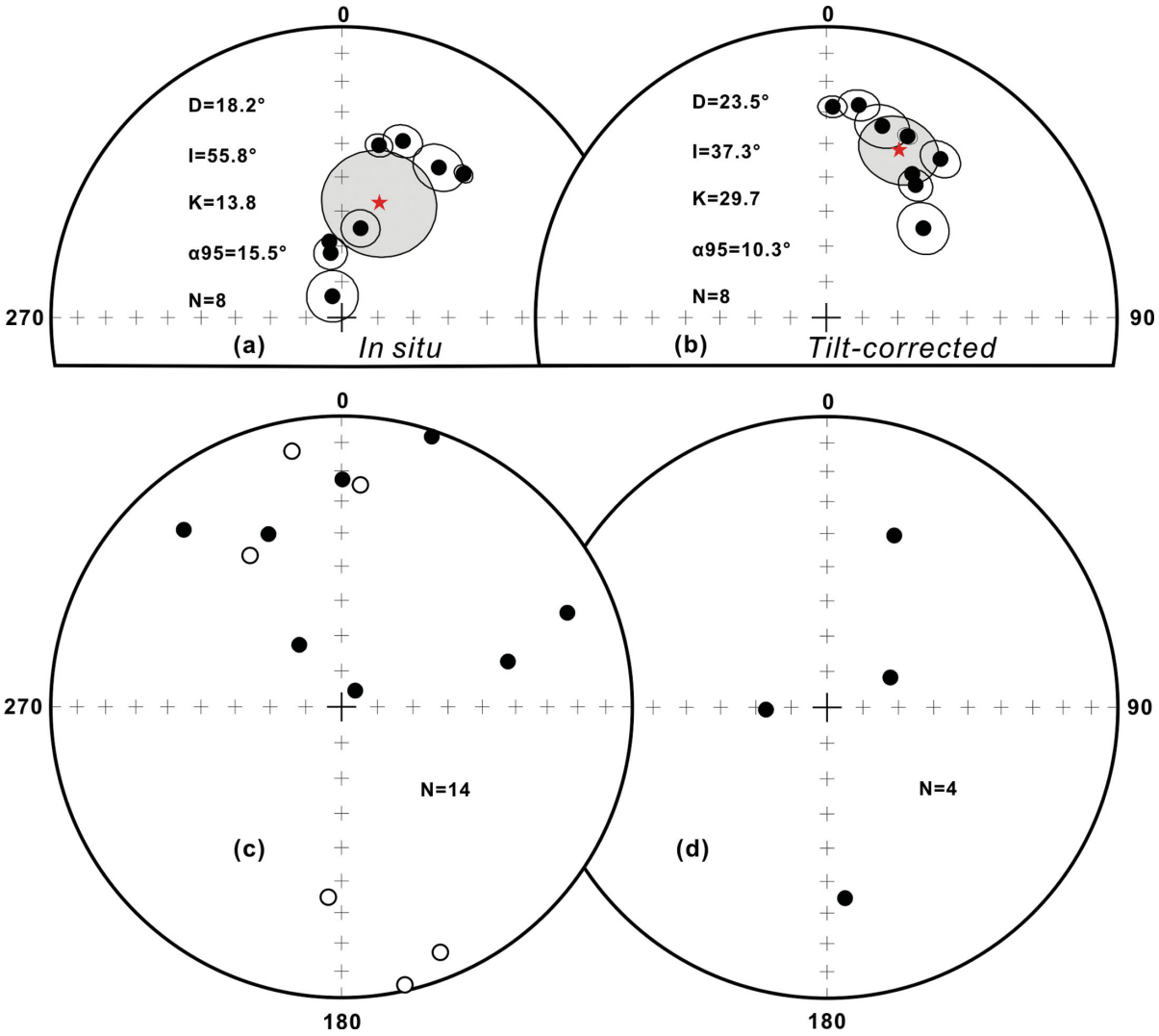

Figure 6. A directional correction fold test (Enkin 2003) of results from basalts in Guangfeng, Jiangxi. Site mean directions from two outcrops are shown in geographic (a) and stratigraphic (b) coordinates. The DC tilt test shows that the maximum clustering occurs at 89 ± 25.9 per cent untilting, suggesting that remanence in the redbeds of Guangfeng area is likely primary in origin. (c) and (d) show the intraformational conglomerate tests at sites JS6 and JS3, respectively. (c) The equal-area projection shows ChRMs of 14 basaltic cobbles in a conglomerate at site JS6 within a sequence of basalt flows. The ChRM directions are randomly distributed, indicating that ChRM was acquired prior to the incorporation of the basaltic pebbles in the conglomerate and basalts retained primary remanent magnetizations. (d) ChRM directions from four redbed fragments at the base of the ∼1-m-thick basalt bed are widely scattered, indicating that remanence in redbeds is likely primary in origin. Open/solid circles are directions in the upper/lower hemisphere.

of Guangxi (Gilder *et al.* 1993) are not used in our analysis as they are thought to have been affected by local deformation. In addition, since high-quality palaeomagnetic data are increasingly reported from South China, it is now possible to reduce uncertainty by placing more stringent criteria in selecting data for regional tectonic interpretation. As such, palaeopoles with A_{95} greater than 10° are excluded.

The remaining reliable Late Cretaceous palaeopoles for South China are shown in Fig. 7(a). One prominent feature is that these palaeopoles are not tightly clustered, but instead appear as two distinct groups; thus, we prefer instead to treat the two subsets separately. To increase the clarity of presentation, these poles are plotted without A_{95} circles (Fig. 7b). Fig. 7(b) shows that one group of palaeopoles occurs at the relatively higher latitudes, or 'H'-position palaeopoles, whereas the other group stands about 10° away at somewhat lower latitudes and are 'L'-position palaeopoles (Table 2).

The separation of these two groups of palaeopoles may represent either the apparent polar wander in the Late Cretaceous or arise from intracontinental deformation within the SCB. The Late Cretaceous portion of the apparent polar wander path (APWP) of Europe, which is commonly used as a reference when it comes to discussing the tectonics of Asia, is characterized by a small loop for the period of 100–60 Ma (Fig. 7c). To examine whether the separation of the two groups of palaeopoles represents a systematic shift from the early Late Cretaceous palaeopoles to the late Late Cretaceous palaeopoles, we further refine the ages of these palaeopoles by taking advantage of the occurrence of the major polarity switch from normal to reverse at around 83 Ma during the Late Cretaceous. Palaeopoles that were determined without the reversed polarity data are considered to be older than 83 Ma and are marked as '83+'. Accordingly, palaeopoles that were determined with results including the reversed polarity data are believed to be younger than 83 Ma and are labelled as '83−'. Though this treatment is somewhat

Table 1. Summary of the palaeomagnetic results from Guangfeng and Jiangshan area, the SCB.

Site no.	Slat	Slong	Lithology	Strike	Dip	*n*/*N*	Dg	Ig	Ds	Is	*k*	α_{95}
Guangfeng												
GF1	28.44	118.17	Basalt	220	24	18/19	40.3	35.5	24.1	32.2	187.1	2.5
GF2	28.44	118.16	Basalt	220	24	8/9	32.9	38.5	16.3	32.0	68.1	6.8
GF3	28.44	118.16	Basalt	222	19	13/13	19.1	36.0	8.7	27.0	70.9	5.0
GF4	28.44	118.16	Diabase dyke	222	19	6/6	12.2	39.3	1.7	28.3	364.0	3.5
GF6	28.29	118.36	Basalt	328	36	12/12	336.3	83.5	47.4	52.6	37.7	7.2
GF7	28.29	118.36	Basalt	328	36	20/20	350.8	68.4	30.9	41.9	277.6	2.0
GF8	28.30	118.35	Basalt	328	36	10/12	11.9	64.4	35.8	33.3	84.3	5.3
GF9	28.30	118.35	Basalt	328	36	11/11	350.1	71.7	34.0	44.3	100.5	4.6
GF10	28.30	118.35	Redbeds	328	36	11/13	10.1	65.9	36.2	35.3	30.8	8.4
GF11	28.31	118.31	Redbeds	330	36	11/11	354.4	59.1	25.3	34.7	81.9	5.1
GF12	28.30	118.35	Redbeds	332	39	5/5	348.4	67.0	32.6	40.2	156.0	6.1
Jiangshan												
JS1	28.61	118.55	Redbeds	250	30	17/18	38.7	53.1	17.5	32.4	388.0	1.8
JS2	28.61	118.55	Basalt	250	30	14/14	31.7	66.5	5.0	42.1	43.3	6.1
JS3	28.61	118.55	Redbed lens			4/4	(conglomerate test)					
JS4	28.61	118.55	Redbeds	248	34	27/28	36.8	59.3	9.9	34.4	131.0	2.4
JS5	28.61	118.55	Basalt	248	35	11/11	32.8	61.8	5.9	34.4	421.9	2.2
JS6	28.60	118.52	Basaltic pebbles			14/14	(conglomerate test)					
JS7	28.61	118.55	Basalt	250	30	9/9	10.9	68.2	354.4	40.1	457.0	2.4
JS8	28.61	118.55	Redbeds	228	37	9/9	37.5	52.2	4.9	34.3	279.0	3.1
Mean redbeds						6	20.6	61.1			39.5	10.8
									20.9	35.8	60.0	8.7
Mean basalts						11	19.9	58.7			18.0	11.1
									17.6	38.1	29.1	8.6
Mean basalts + red beds							20.1	59.6			23.3	7.5
	28.4	118.3				17			18.8	37.3	36.9	6.0

Note: Strike and dip are bedding attitudes following the right-hand rule; *n/N*, number of samples used to calculate the mean ChRMs/number of demagnetized samples; Dg and Ig, declination and inclination in geographic coordinates, respectively; Ds and Is, declination and inclination in stratigraphic coordinates, respectively; *k*, Fisher's (1953) precision parameter; α_{95}, radius of 95 per cent confidence. All angles are in degrees.

imprecise, it represents an improved refinement of the ages of these palaeopoles. This treatment is necessary because tight age control of these palaeopoles becomes equally important to the reliability of these palaeopoles for deciphering the separation of palaeopoles that were obtained from one tectonic unit, i.e. the SCB, within such a short period of time, i.e. Late Cretaceous from 100 to 65 Ma. The '83+'-aged palaeopoles and the '83−' -aged palaeopoles are plotted in Fig. 7(d). It is evident that the '83+'-aged palaeopoles occur in both the 'L'-position and the 'H'-positions, implying that the separation between the 'L'-position palaeopoles and the 'H'-position palaeopoles may not result from the Late Cretaceous apparent polar wander.

To investigate the second possible cause of separation of these palaeopoles, i.e. intracontinental deformation within the SCB, the relationship between the palaeopole positions and the locations from which these palaeopoles were obtained (Fig. 7e). The 'H'-position palaeopoles and the 'L'-position palaeopoles are represented by squares and triangles, respectively, in the location map (Fig. 7e). It is evident that the majority of the 'H'-position palaeopoles are from the fault-bounded southwestern and southeastern margins of the SCB (Fig. 7e). The six 'H'-position palaeopoles from the fault-bounded SW and SE margins of the SCB yield a mean pole at $P_{\text{lat.}} = 81.5^\circ$, $P_{\text{long.}} = 193.7^\circ$ with $A_{95} = 3.2^\circ$. It is also clear that the majority of the 'L'-position palaeopoles are from stable central SCB (Fig. 7e). The six 'L'-position palaeopoles from the inland SCB produce a mean pole at 72.3°N, 235.6°E and $A_{95} = 3.1^\circ$ (Table 2). Overall evidence appears to weigh towards the deformational cause of the separation of these poles.

6.2 Inclination shallowing or crustal deformation in South China?

Basalts and redbeds from the Jiangshan–Guangfeng area yield similar inclinations (Table 1), suggesting that sampled redbeds did not suffer inclination shallowing. In addition, the palaeomagnetic results of basalts from the Jiangshan–Guangfeng area produce a palaeopole at 72.6°N, 228.1°E, $A_{95} = 7.8^\circ$, which is almost identical to the redbed palaeopole from the nearby Ganzhou area in Jiangxi Province (74.4°N, 225.1°E, $A_{95} = 5.2^\circ$) (Wang & Yang 2007), attesting that redbeds in Jiangxi do not suffer inclination shallowing. Indeed, all currently available three igneous-derived palaeopoles from the SCB including the basalts-derived palaeopole from Guangfeng–Jiangshan area (this study), the intrusive-derived palaeopole from Hong Kong (Li *et al.* 2005), and the basalts-derived palaeopole from Fujian (Huang *et al.* 2013), largely overlap the redbed-derived palaeopoles from South China (Fig. 7a), indicating the first-order consistency in palaeomagnetic results from the SCB redbeds and volcanics. Although these Late Cretaceous poles are not tightly clustered and appear to emerge as two distinct groups, namely the 'L'-position group and the 'H'-position group, reasonable consistency exists within each group between volcanic- and redbed-derived palaeopoles (Figs 7a and b). Collectively, comparison of palaeomagnetic data from volcanic rocks and redbeds at various scales appears to persistently suggest that palaeomagnetic results from the two types of rocks agree reasonably well, thus arguing for no significant inclination shallowing of redbeds in the SCB.

Table 2. Summary of Late Cretaceous palaeomagnetic pole data from the SCB.

Study area	Rock type	Age[d]	S_{Lat}	S_{Long}	P_{Lat}	P_{Long}	A_{95}	Q	References	Remarks
Jiangshan–Guangfeng	Redbeds	83+	28.4	118.3	69.0	228.1	10.0	6	This study	
Jiangshan–Guangfeng	Basalts	83+	28.4	118.3	72.3	226.2	9.5	6	This study	
Jiangshan–Guangfeng	Basalts+redbeds	83+	28.4	118.3	71.1	226.9	6	6	This study	Poles at
Ganzhou, Jiangxi	Redbeds	83−	25.9	114.9	74.4	225.1	5.2	7	Wang & Yang (2007)	Low-latitude
Hengyang, Hunan	Redbeds	83−	26.9	112.6	71.9	236.3	4.7	7	Sun *et al.* (2006)	postions
Yichang, Hubei	Redbeds	83+	30.7	111.7	71.7	254.1	5.6	7	Narumoto *et al.* (2006)	('L')
Hong Kong	Dykes	83−	22.2	114.1	69.3	211.2	8.9	6	Li *et al.(* 2005)	
Central Sichuan	Redbeds	83−	30.0	102.9	72.8	241.1	6.6	5	Enkin *et al.* (1991)	
Zhejiang	Redbeds	83+	28.8	119.8	81.0	214.3	6.4	6	Morinaga & Liu (2004)	
Fujian	Redbeds	83+	25.9	117.2	79.7	201.7	5.8	6	Morinaga & Liu (2004)	
Guangdong	Redbeds	83+	24.1	115.4	80.8	177.7	8.0	6	Morinaga & Liu (2004)	Poles at
Pan-Xi, SW Sichuan	Redbeds	83+	26.6	102.4	78.9	186.6	5.4	5	Zhu *et al.* (1988)	High-latitude
Southwestern Sichuan	Redbeds	83+	26.5	102.4	81.5	220.9	7.1	7	Huang & Opdyke (1992)	postions
western Hunan	Redbeds	83+	28.2	110.2	83.5	168.1	4.0	6	Zhu *et al.* (2006)	('H')
Yongtai, Fujian	Volcanic rocks	83+	25.7	119.0	83.1	152.5	3.9	5	Huang *et al.* (2013)	
Jishui, Jiangxi[a]	Redbeds		27.2	115.1	81.0	322.2	5.8	6	Wang & Yang (2007)	Local rotation
Qinzhou, Guangxi[a]	Redbeds		22.2	108.7	79.4	7.1	10.0	5	Gilder *et al.* (1993)	Local rotation
Nanjing, Jiangsu[a]	Purple sandstone		32.0	119.0	76.3	172.6	10.3	6	Kent *et al.* (1986)	$A_{95}>10$
Anhui[a]	Purple siltstone		30.8	118.2	83.8	200.3	14.6	7	Gilder *et al.* (1999)	$A_{95}>10$
Mean of redbeds ($N=11$)					77.9	221.8	4.2		This study	
Mean of volcanics ($N=3$)					76.2	209.3	16.0		This study	
Mean of 'L'-position poles ($N=7$)					72.1	231.3	3.5		This study	
Mean of 'H'-position poles ($N=7$)					81.8	190.9	2.9		This study	
Mean of poles from inland South China ($N=6$)[b]					72.3	235.2	3.2		This study	
Mean of poles from SE and SW margins of South China ($N=6$)[c]					81.5	193.7	3.2		This study	
Mean 70–100 Ma Eurasia reference pole ($N=4$)					81.5	198.5	2.2		Besse & Courtillot 2002	

Notes: S_{Lat} and S_{Long} are the latitude and longitude of study sites, respectively; P_{lat} and P_{long} are the latitude and longitude of poles; A_{95} is the 95 per cent confidence angle of poles; Q is the reliability index of palaeomagnetic data following Van der Voo (1990). All angles are in degree.

[a]Poles from these areas are excluded for discussions of regional tectoncis because these poles were either affected by local rotations or have an $A_{95} > 10$;

[b]'L'-position poles except the one from Hong Kong,

[c]'H'-position poles except the one from western Hunan, see Fig. 7 and text for details.

[d]The age of these late Cretaceous poles is further refined based on the presence and absence of reversed polarities. Poles with reversed polarities are considered younger than 83 Ma, the termination age of the Cretacous Long Normal Polarity zone, and are denoted as '83−'. Accordingly, poles without reversed polarities are considered older than 83 Ma and are denoted as '83+'.

Previous studies show that poles that were obtained from central part of the SCB including Ganzhou (Wang & Yang 2007), Yichang (Narumoto *et al.* 2006) and Hengyang (Sun *et al.* 2006) are separated from a reference pole of Europe and are located far-sided with respect to the reference pole. This far-sided separation of these poles was attributed to inclination shallowing of the redbeds in central part of South China (e.g. Narumoto *et al.* 2006; Sun *et al.* 2006; Wang & Yang 2007). As discussed above, volcanic rocks and redbeds yield largely consistent palaeomagnetic results, which appear to suggest no significant inclination shallowing of redbeds. Therefore, the approach that involves comparing palaeopoles with a reference pole needs to be scrutinized and the significance of a separation of palaeopoles from a reference pole, if any, needs to be re-examined.

When choosing a reference pole of Eurasia, a common practice is to select a pole with an age similar to that of the studied rocks. However, comparisons are often made between poles with wider age windows (e.g. spanning the entire Late Cretaceous) from the SCB and the reference pole with a typical narrow sliding age window (e.g. 10 or 20 Myr), a practice that may introduce errors for the comparison. Therefore, instead of choosing the 95 Ma pole as a reference pole, we take the average of the 70–100 Ma poles of Europe (Besse & Courtillot 2002) as a reference pole (81.5°N, 198.5°E, $A_{95} = 2.2°$) for the Late Cretaceous.

The Late Cretaceous palaeopoles from the SCB are compared with this newly defined reference pole to examine their significance (Fig. 8). The 'L'-position palaeopoles are clearly separated from the reference pole and is located far-sided with respect to the reference pole (Fig. 8). Since these 'L'-position poles are mainly from inland SCB, the previously observed far-sided separation of redbeds-derived palaeopoles from a reference pole remains despite of the improved definition of the reference pole. The far-sided separation between the mean of these coherent 'L'-position palaeopoles from the inland SCB with the newly defined reference pole of Europe amounts to $10.8° \pm 2.8°$ in palaeolatitude and a minor clockwise rotation ($5.8° \pm 3.0°$). Because inclination shallowing of redbeds appears not to be an issue, the remained far-sided separation of redbeds from inland SCB raises intriguing questions as to the causes of this far-sided problem. The far-sided separation cannot be due to tectonic shortening between the SCB and its northern blocks including the NCB, Amuria and Siberia blocks. The SCB and NCB sutured by Late Jurassic (Zhao & Coe 1987; Enkin *et al.* 1992; Gilder & Courtillot 1997; Yang & Besse 2001). The NCB accreted to Amuria by the Late Carboniferous (Zonenshain *et al.* 1990). The Mongol–Okhotsk Ocean that separates Amuria and Siberia closed by the Late Jurassic–Early Cretaceous (Zorin 1999; Kravchinsky *et al.* 2002; Cogné *et al.* 2005). A non-dipolar field or persistent qudrapole and octupole field was considered another possible cause for the

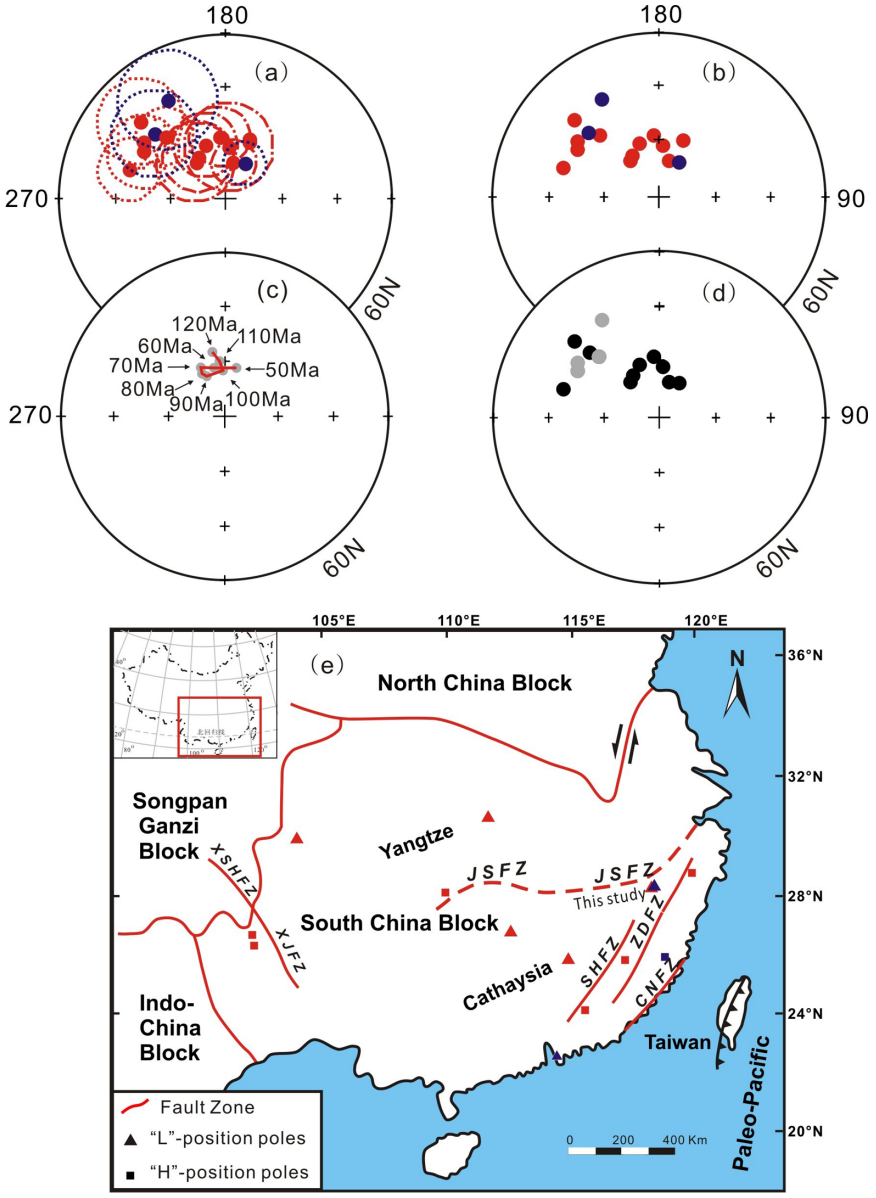

Figure 7. Selected Late Cretaceous palaeopoles of the SCB (see text). The palaeopoles are shown with (a) and without (b) 95 per cent confidence circles. Red and purple solid circles represent palaeopoles from redbeds and volcanic rocks, respectively. The late Cretaceous APWP of Europe is shown in (c). The Late Cretaceous palaeopoles are reclassified according to whether they are greater (83+, black) or less (83-, grey) than 83 Ma (d). The locations where these Late Cretaceous poles were obtained are shown in (e). Squares and triangles denote the 'H'- and 'L'-position palaeopoles, respectively, and red and purple colours indicate palaeopoles that were derived from redbeds and volcanic rocks, respectively, in (e). JSFZ, Jiangshan-Shaoxing Fault Zone; SHFZ, Shaowu-Heyuan Fault Zone; ZDFZ, Zhenghe-Dapu Fault Zone; CNFZ, Changle-Nanao Fault Zone; XSHFZ, Xianshuihe Fault Zone; XJFZ, Xiaojiang Fault Zone.

far-sided problem (Si & Van der Voo 2001; van der Voo & Torsvik 2001; Torsvik & Van der Voo 2002). However, the qudrapole field is estimated to contribute to only 3 per cent of the geomagnetic field over the past 200 Myr, which only accounts for 1.4 ± 1.2°far-sided offset (Besse & Courtillot 2002; Courtillot & Besse 2004). The non-rigidity of the Eurasia plate was postulated as a third possible cause of the Cenozoic far-sided separation of East Asia palaeopoles and the Europe reference pole (Cogné *et al.* 1999). In this hypothesis, the huge, rigid, mega-plate of Eurasia was formed by the Cretaceous (Hankard *et al.* 2007a, 2008). However, Eurasia plate did not behave as a single rigid block in the Cenozoic such that the eastern Eurasia blocks was located about 10° south of the expected latitudes (Cogné *et al.* 1999; Hankard *et al.* 2007b). The non-rigid deformation of Eurasia was accommodated via relative movements along the Tornquist–Tesseyre line and the Ural Mountains (Cogné *et al.* 2013). Palaeomagnetic data from the Eocene rocks from the SCB show a 12.8 ± 4.0° far-sided separation from the corresponding reference pole (Sun *et al.* 2006), thus supporting the non-rigidity hypothesis. Unlike the Cretaceous palaeopoles from its northern blocks including NCB, Amuria and Siberia that are consistent with the Europe reference pole, the Late Cretaceous palaeopoles of the inland SCB are situated far-sided with respect to the Europe reference pole (Fig. 8). This may raise the possibility that the SCB was decoupled with its northern blocks, which is tectonically paradoxical and can only be resolved with more high-quality, well-dated palaeomagnetic data from these blocks. Despite this, the far-sided feature of the Late Cretaceous 'L'-position palaeopoles of the SCB is consistent in nature and compatible in magnitude with that of the

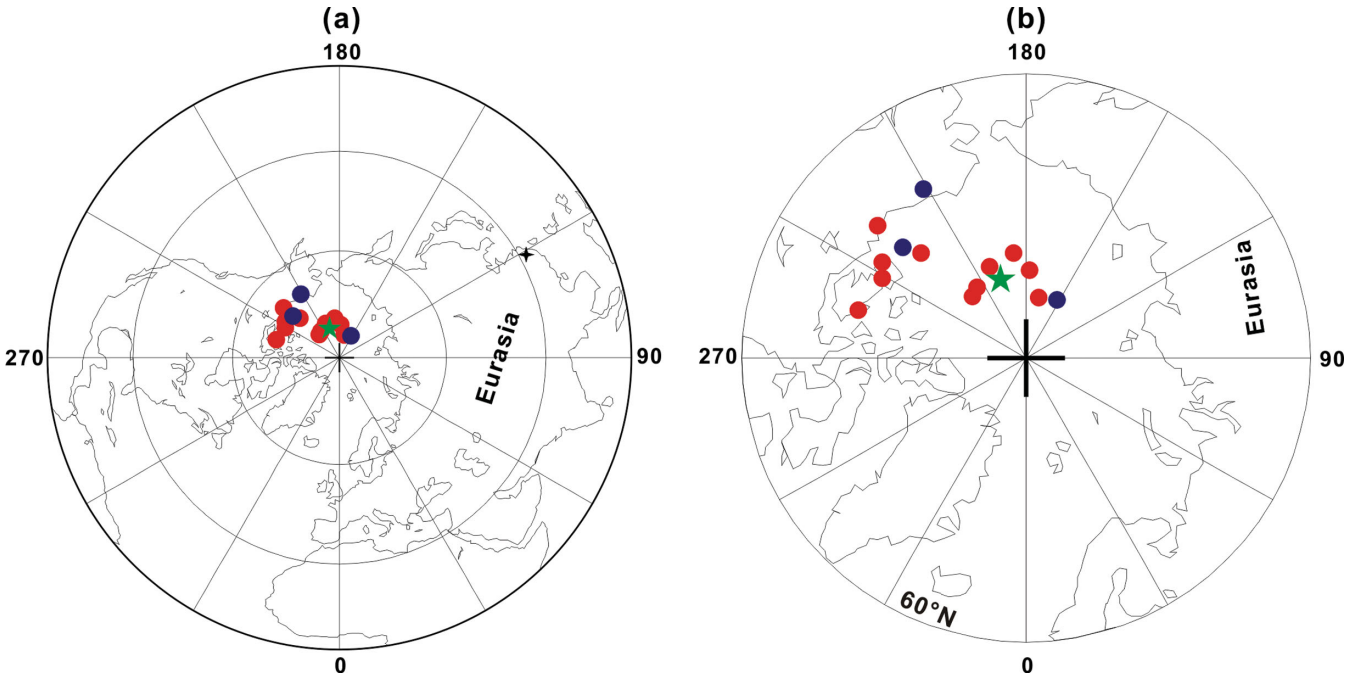

Figure 8. Comparison of the Late Cretaceous palaeopoles of the SCB and the reference pole of Europe (a, b). Colour scheme is same as that in Fig. 7. The reference pole of Europe is marked by the asterisk and is obtained by averaging the 70–100 Ma poles of Europe. Note that (b) is a close-up view of the palaeopole positions shown in (a) and its circumference is 60°N, not equator as shown in (a).

Eocene rocks of the SCB. This similar feature in the Cretaceous and the Cenozoic likely resulted from the non-rigid deformation of the Eurasia plate in the Cenozoic that displaced the relatively older, i.e. Cretaceous, palaeoples in a similar fashion. As such, the $10.8^\circ \pm 2.8^\circ$ far-sided separation of the 'L'-position palaeopoles is best interpreted as indicating the nonrigid nature of the Eurasia plate without invoking an over 1000 km poleward tectonic displacement that was not seen in geological data. The minor clockwise rotation of $5.8^\circ \pm 3.0^\circ$ can be explained by the eastward movement of the SCB with respect to Europe in response to the Cenozoic India–Asia collision.

The 'H'-position palaeopoles, which are mainly from the fault-bounded SW and SE margins of the SCB, are closely grouped around the reference pole, indicating no significant displacement with respect to Europe. However, comparison of palaeopoles from the SW and SE margins with those of the stable central part of the SCB indicates a $5.9^\circ \pm 3.6^\circ$ clockwise rotation and a $-11.5^\circ \pm 3.3^\circ$ poleward offset. For palaeopoles from the southwest SCB, the indicated block rotation and displacement may result from the NW-trending, left-lateral, strike-slip faulting (e.g. Xianshuihe fault, Fig. 7e) that led to the southeastward movement of blocks in response to the Cenozoic India–Asia collision. For palaeopoles from the SE coastal margin, the results can be explained by dextral shear along the coast-parallel faults such as Heyuan–Shaowu fault, Zhenghe–Dapu fault and Changle–Nanao fault (Fig. 7e) and widespread lithospheric extension (Li 2000) that moved blocks in the coastal margins away relative to the central part of the SCB. The dextral strike-slip is well documented in deformed rocks adjacent to the coast-parallel faults (Charvet *et al.* 1990; Shu *et al.* 2000). The minor clockwise rotation of blocks in these areas could result from the combined effect of the eastward movement of these blocks associated with the India–Asia collision and the intensified extension related to the subduction of the proto-Pacific plate.

7 CONCLUSIONS

We draw the following conclusions based on our palaeomagnetic study of the Upper Cretaceous (~95 Ma) basalts and redbeds from the Jiangshan–Guangfeng area of southeastern China and the analyses of the Late Cretaceous palaeopoles of both the SCB and Europe.

(1) This study shows that basalts and redbeds record primary remanences and carry statistically indistinguishable directions (the redbed one is at 69.0°N, 228.1°E, $A_{95} = 10.0^\circ$, while the basalt one is at 72.3°N, 226.2°E, $A_{95} = 9.5^\circ$).

(2) Critical examination of Late Cretaceous palaeopoles of the SCB has led us making a new compilation based on 14 reliable palaeopoles (11 from redbed and 3 from volcanic). Overall, the volcanic palaeopoles overlap the redbed palaeopoles. Also, the poles from South China are not tightly clustered and appear as two separate groups, one at relatively high latitudes, i.e. 'H'-position poles and the other at relatively lower degrees i.e. 'L'-position poles. Within each group, reasonable consistency exists between volcanics-derived palaeopoles and redbeds-derived palaeopoles. The similarity in palaeopoles of redbeds and volcanic rocks at different levels suggests that redbeds in the SCB do not suffer significant inclination shallowing.

(3) Investigation of the cause for the separation of the 'H'-position palaeopoles and 'L'-position paleopoles suggests that it is not due to apparent polar wander, but instead crustal deformation. The 'H'-position paleopoles are mainly from the central SCB and the 'L'-position palaeopoles are mainly from the fault-bounded SW and SE margins of the SCB.

(4) Comparison of the reliable Late Cretaceous palaeopoles with the reference pole of Europe, which is defined as the mean of the 70–90 Ma poles of Europe, shows that palaeopoles from redbeds in central part of the SCB are separated by ~11° from the reference pole. Since redbeds in the SCB do not appear to have suffered significant inclination shallowing and ~1200 km displacement of

the SCB relative to Europe appears unlikely, the $\sim 11^\circ$ separation can be best explained by the non-rigidity of Eurasia plate. As such, a reference pole for the SCB is defined at 72.3°N, 235.2°E with $A_{95} = 3.2^\circ$ based on six palaeopoles from stable central SCB that suggest that the core of the block has behaved as a coherent body since the Late Cretaceous.

ACKNOWLEDGEMENTS

This study was supported by a grant from the State Key Laboratory for Mineral Deposits Research (Nanjing University). YXL gratefully acknowledges the support from the New Century Excellent Talent in University Awards from the Ministry of Education, China (NCET-09-0457). Chen Xijie and Wang Shipeng are thanked for field assistance. This paper also benefited from discussions with Xiaodong Tan and Yan Chen. An anonymous reviewer and Jean-Pascal Cogné are thanked for providing critical and constructive comments on an early version of the manuscript that helped improve the paper.

REFERENCES

Ali, J.R., Lo, C.H., Thompson, G.M. & Song, X.Y., 2004. Emeishan Basalt Ar-Ar overprint ages define several tectonic events that affected the western Yangtze platform in the Mesozoic and Cenozoic, *J. Asian Earth Sci.,* **23,** 163–178.

Besse, J. & Courtillot, V., 2002. Apparent and true polar wander and the geometry of the geomagnetic field over the last 200 Myr, *J. geophys. Res.,* **107**(B11) 2300, doi:10.1029/2000JB000050.

Bilardello, D. & Kodama, K.P., 2010. Paleomagnetism and magnetic anisotropy of Carboniferous red beds from the Maritime Provinces of Canada: evidence for shallow paleomagnetic inclinations and implications for North American apparent polar wander, *Geophys. J. Int.,* **180,** 1013–1029.

Bureau of Geology and Mineral Resources of Zhejiang Province, 1996. *Rocks and Formations in Zhejiang Province,* pp. 236, Publishing House of China University of Geosciences, Beijing, China (in Chinese).

Cai, Z.Q. & Yu, Y.W., 2001. Subdivision and correlation of the upper beds of the Cretaceous system in Zhejiang, *J. Stratigraphy,* **25,** 259–266 (in Chinese with English abstract).

Charvet, J., Cluzel, D. & Faure, M., 1999. Some tectonic aspects of the pre-Jurassic accretionary evolution of East Asia, in *Gondwana Dispersion and Asian Accretion,* pp. 37–65, eds Metcalfe, I., Ren, J., Charvet, J. & Hada, S., A. A. Balkema, Rotterdam/Brookfield.

Charvet, J., Faure, M., Xu, J.W., Zhu, G., Tong, W.X. & Lin, S.F., 1990. La zone tectonique de Changle-Nanao, Chine du sud-est, *C R Acad. Sci. Paris,* **t310,** 1271–1278.

Charvet, J., Shu, L.S., Faure, M., Choulet, F., Wang, B., Lu, H.F. & Le Breton, N., 2010. Structural development of the Lower Paleozoic belt of South China: genesis of an intracontinental orogen, *J. Asian Earth Sci.,* **39,** 309–330.

Charvet, J., Shu, L.S., Shi, Y.S., Guo, L.Z. & Faure, M., 1996. The building of South China: collision of Yangzi and Cathaysia block, problems and tentative answers, *J. Southeast Asian Earth Sci.,* **13,** 223–235.

Chen, Y., Cogné, J-P. & Courtillot, V., 1992. New Cretaceous paleomagnetic poles from the Tarim Basin, northwestern China, *Earth planet. Sci. Lett.,* **114,** 17–38.

Cogné, J.P., 2003. PaleoMac: a Macintosh^{TM} application for treating paleomagnetic data and making plate reconstructions, *Geochem. Geophys. Geosyst.,* **4**(1), 1007, doi:10.1029/2001GC000227.

Cogné, J.P., Halim, N., Chen, Y. & Courtillot, V., 1999. Resolving the problem of shallow magnetizations of Tertiary age in Asia: insights from paleomagnetic data from the Qiangtang, Kunlun, and Qaidam blocks (Tibet, China), and a new hypothesis, *J. geophys. Res.,* **104B,** 17 715–17 734.

Cogné, J.P., Kravchinsky, V.A., Halim, N. & Hankard, F., 2005. Late Jurassic-Early Cretaceous closure of the Mongol-Okhotsk Ocean demonstrated by new Mesozoic paleomagnetic results from the Trans-Baïkal area (SE Siberia), *Geophys. J. Int.,* **163,** 813–832.

Cogné, J.-P., Besse, J., Chen, Y. & Hankard, F., 2013. A new Late Cretaceous to Present APWP for Asia and its implications for paleomagnetic shallow inclinations in Central Asia and Cenozoic Eurasian plate deformation, *Geophys. J. Int.,* doi:10.1093/gji/ggs104.

Courtillot, V. & Besse, J., 2004. A long-term octupolar component in the geomagnetic field? (0–200 million years B.P.), in *Timescales of the Palaeomagnetic Field,* Geophysical Monograph Series, Vol. 145, pp. 59–74, eds Channell, J.E.T., Kent, D.V., Lowrie, W. & Meert, J., AGU, Washington, DC.

Cui, Y.R., Xie, Z., Wang, B., Chen, J.F., Yu, Y.W. & He, J.F., 2011. Geochemical characteristics of the Late Mesozoic basalts in Southeastern Zhejiang Province and constraints on magma source materials, *Geol. J. China Univ.,* **17,** 492–512.

Enkin, J.R., Courtillot, V., Xing, L., Zhang, Z., Zhuang, Z. & Zhang, J., 1991. The stationary Cretaceous paleomagnetic pole of Sichuan (South China Block), *Tectonics,* **10,** 547–559.

Enkin, R.J., 2003. The direction-correction tilt test: an all-purpose tilt/fold test for paleomagnetic studies, *Earth planet. Sci. Lett.,* **212,** 151–166.

Enkin, R.J., Yang, Z.Y. & Courtillot, V., 1992. Paleomagnetic constraints on the geodyanmic history of the major blocks of China from the Permian to the present, *J. geophys. Res.,* **97**(13), 953–989.

Finlay, C.C. *et al.*, 2010. International geomagnetic reference field: the eleventh generation. International Association of Geomagnetism and Aeronomy, Working Group V-MOD, *Geophys. J. Int.,* **183**(3), 1216–1230.

Fisher, R.A., 1953. Dispersion on a sphere, *Proc. R. Soc. Lond.,* **A 217,** 295–305.

Funahara, S., Nishiwaki, N., Miki, M., Murata, F., Otofuji, Y. & Wang, Y.Z., 1992. Paleomagnetic study of Cretaceous rocks from the Yangtze block, central Yunnan, China: implications for the India-Asia collision, *Earth planet. Sci. Lett.,* **113,** 77–91.

Gareces, M., Pares, J.M. & Cabrera, L., 1996. Further evidence for inclination shallowing in redbeds, *Geophys. Res. Lett.,* **23,** 2065–2068.

Gilder, S. & Courtillot, V., 1997. Timing of the north-south China collision from new middle to late Mesozoic paleomagnetic data from the North China block, *J. geophys. Res.,* **102,** 17 713–17 727.

Gilder, S., Chen, Y. & Sen, S., 2001. Oligo-Miocene magnetostratigraphy and rock magnetism of the Xishuigou section, Subei (Gansu Province, western China) and implications for shallow inclinations in central Asia, *J. geophys. Res.,* **106**(12), 30 505–30 521.

Gilder, S.A., Chen, Y., Cogné, J.-P., Tan, X., Courtillot, V., Sun, D. & Li, Y., 2003. Paleomagnetism of Upper Jurassic to Lower Cretaceous volcanic and sedimentary rocks from the western Tarim Basin and implications for inclination shallowing and absolute dating of the M-0 (ISEA?) chron, *Earth planet. Sci. Lett.,* **206,** 587–600.

Gilder, S.A., Coe, R.S., Wu, H.R., Kuang, G.D., Zhao, X.X., Wu, Q. & Tang, X.Z., 1993. Cretaceous and Tertiary paleomagnetic results from southeast China and their tectonic implications, *Earth planet. Sci. Lett.,* **117,** 637–652.

Gilder, S.A., Keller, R.G., Luo, M. & Goodell, P.C., 1991. Timing and spatial distribution of rifting in China, *Tectonophysics,* **197,** 225–243.

Gilder, S.A. *et al.*, 1996. Isotopic and paleomagnetic constraints on the Mesozoic tectonic evolution of south China, *J. geophys. Res.,* **101,** 16 137–16 154.

Gilder, S.A. *et al.*, 1999. Tectonic evolution of Tancheng-Lujiang (Tan-Lu) Fault via Middle Triassic to Early Cenozoic paleomagnetic data, *J. geophys. Res.,* **104,** 15 365–15 390.

Gu, X.L. & Gu, W., 1990. Paleomagnetism and tectonic implication of the Late Cretaceous Red' Bed in the Ji-tai Basin, South China, *Abstracts for the 4th National Symposium on Paleomagnetism,* Zhejiang University, Hangzhou, China, 22 pp. (in Chinese).

Guo, L.Z., Shi, Y.S., Lu, H.F., Ma, R.S., Dong, H.G. & Yang, S.F., 1989. The pre-Devonian tectonic patterns and evolution of South China, *J. Southeast Asian Earth Sci.,* **3,** 87–93.

Hankard, F., Cogné, J.P., Quidelleur, X., Bayasgalan, A. & Lkhagvadorj, P., 2007a. Paleomagnetism and K-Ar dating of Cretaceous basalts from Mongolia, *Geophys. J. Int.,* **169,** 898–908.

Hankard, F., Cogné, J.P., Kravchinsky, V.A., Carporzen, L., Bayasgalan, A. & Lkhagvadorj, P., 2007b. New Tertiary paleomagnetic poles from Mongolia and Siberia at 40, 30, 20 and 13 Ma: clues on the inclination shallowing problem in Central Asia, *J. geophys. Res.,* **112,** B02101.

Hankard, F., Cogné, J.P., Kravchinsky, V.A., Bayasgalan, A. & Lkhagvadorj, P., 2008. Palaeomagnetic results from Palaeocene basalts from Mongolia reveal no inclination shallowing at 60 Ma in Central Asia, *Geophys. J. Int.,* **172,** 87–102.

Hu, L., Li, P. & Ma, X., 1990. A magnetostratigraphic study of Cretaceous Red Beds from Shanghan, western Fujian, China, *Geol. Fujian,* **1,** 33–42 (in Chinese).

Huang, K. & Opdyke, N.D., 1992. Paleomagnetism of Cretaceous to lower Tertiary rocks from southwestern Sichuan: a revisit, *Earth planet. Sci. Lett.,* **112,** 29–40.

Huang, S., Pan, Y.X. & Zhu, R.X., 2013. Paleomagnetism of the Upper Cretaceous volcanic rocks from the Shimaoshan Group in Yongtai County, Fujian (in Chinese), *Sci. China Earth Sci.,* **56,** 22–30.

Ichikawa, K., Mizutani, S. & Hara, I., 1990. *Pre-Cretaceous terrances of Japan. Pre-Jurassic evolution of Eastern Asia,* Osaka, 413 pp.

Kent, D.V., Xu, G., Huang, K., Zhang, W.Y. & Opdyke, N.D., 1986. Paleomagnetism of Upper Cretaceous rocks from South China, *Earth planet. Sci. Lett.,* **79,** 179–184.

Kirschvink, J.L., 1980. The least-square line and plane and the analysis of paleomagnetic data, *Geophys. J. R. astr. Soc.,* **62,** 699–718.

Kravchinsky, V.A., Cogné, J.P., Harbert, W. & Kuzmin, M.I., 2002. Evolution of theMongol-Okhotsk ocean as constrained by new palaeomagnetic data from the Mongol-Okhotsk suture zone, *Geophys. J. Int.,* **148,** 34–57.

Lapierre, H., Jahn, B.M., Charvet, J. & Yu, Y.W., 1997. Mesozoic felsic arc magmatism and continental olivine tholeiites in Zhejiang Province and their relationship with tectonic activity in SE China, *Tectonophysics,* **274,** 321–338.

Li, K., Shen, J. & Wang, X., 1989. The isotopic geochronology of Mesozoic volcanics in Zhejiang, Fujian and Jiangxi Provinces[J], *Bull. Nanjing Inst. Geol. Miner. Resour.,* **5,** 86–136 (in Chinese).

Li, X.H., 2000. Cretaceous magmatism and lithsospheric extension in SE-China, *J. Asian Earth Sci.,* **18,** 293–305.

Li, X.H., Li, W.X., Li, Z.X., Lo, C.H., Wang, J., Ye, M.F. & Yang, Y.H., 2009. Amalgamation between the Yangtze and Cathaysia Blocks in South China: constraints from SHRIMP U–Pb zircon ages, geochemistry and Nd–Hf isotopes of the Shuangxiwu volcanic rocks, *Precambrian Res.,* **174,** 117–128.

Li, Y., Ali, J.R., Chan, L.S. & Lee, C.M., 2005. New and revised set of Cretaceous paleomagnetic poles from Hong Kong: implications for the development of southeast China, *J. Asian Earth Sci.,* **24,** 481–493.

Li, Z.X. & Li, X H., 2007. Formation of the 1300-km-wide intracontinental orogen and postorogenic magmatic province in Mesozoic South China: a flat-slab subduction model, *Geology,* **35,** 179–182.

Li, Z.X., 1998. Tectonic history of the major East Asia lithospheric blocks since the Mid-Proterozoic—a synthesis, in *Mantle Dynamics and Plate Interactions in East Asia,* Geodynamics Series No 27, Vol. 27, pp. 221–243, eds Flower, M., Chung, S.L., Lee, T.Y. & Lo, C.H., AGU, Washington, DC.

Liu, Y.Y. & Morinaga, H., 1999. Cretaceous paleomagnetic results from Hainan Island in south China supporting the extrusion model of Southeast Asia, *Tectonophysics,* **301,** 133–144.

Liu, Y.Y., Tian, W.H. & Zhu, Y.M., 1999. Paleomagnetic study of Cretaceous basin I at Lishui, Zhejiang Province, *Earth Sci. J. China Univ. Geosci.,* **24,** 139–141 (in Chinese with English abstract).

Lo, C.H. & Yui, T.H., 1996. $^{40}Ar/^{39}Ar$ dating of high-pressure rocks in the Tananao basement complex, Taiwan, *J. Geol. Soc. China,* **39,** 13–30.

Lowrie, W., 1990. Identification of ferromagnetic minerals in a rock by coercivity and unblocking temperature properties, *Geophys. Res. Lett.,* **17,** 159–162.

Ma, X., Yang, Z. & Xing, L., 1993. The lower Cretaceous reference pole for North China, and its tectonic implications, *Geophys. J. Int.,* **115,** 323–331.

McFadden, P.L., Merrill, R.T., McElhinny, M.W. & Lee, S.H., 1991. Reversals of the Earth's magnetic field and temporal variations of the dynamo families, *J. geophys. Res.,* **96B,** 3923–3933.

Metcalfe, I., 1996. Gondwanaland dispersion, Asia accretion and evolution of Eastern Tethys, *Aust. J. Earth Sci.,* **43,** 605–623.

Metcalfe, I., 2002. Permian tectonic framework and paleogeography of SE Asia, *J. Asian Earth Sci.,* **20,** 551–566.

Morinaga, H. & Liu, Y., 2004. Cretaceous paleomagnetism of the eastern South China Block: establishment of the stable body of SCB, *Earth planet. Sci. Lett.,* **222,** 971–988.

Narumoto, K., Yang, Z., Takemoto, K., Zaman, H., Morinaga, H. & Otofuji, Y., 2006. Anomalously shallow inclination in middle-northern part of the South China block: palaeomagnetic study of Late Cretaceous redbeds from Yichang area, *Geophys. J. Int.,* **164,** 290–300.

Otofuji, Y., Liu, Y., Yokoyama, M., Tamai, M. & Yin, J., 1998. Tectonic deformation of the southwestern part of the Yangtze craton inferred from paleomagnetism, *Earth planet. Sci. Lett.,* **156,** 47–60.

Otofuji, Y.-I., Yokoyama, M., Kitada, K. & Zaman, H., 2010. Paleomagnetic versus GPS determined tectonic rotation around eastern Himalayan syntaxis in East Asia, *J. Asian Earth Sci.,* **37,** 438–451.

Ren, J., Tamaki, K., Li, S. & Zhang, J., 2002. Late Mesozoic and Cenozoic rifting and its dynamic setting in Eastern China and adjacent areas, *Tectonophysics,* **344,** 175–205.

Sato, S.Z., Yang, Y., Tong, Y.B., Fujihara, M., Zaman, H., Yokoyama, M., Kitada, K. & Otofuji, Y., 2011. Inclination variation in the Late Jurassic to Eocene red beds from southeast Asia: lithological to locality scale approach, *Geophys. J. Int.,* **186,** 471–491.

Shu, L.S. & Charvet, J., 1996. Kinematic and geochronology of the Proterozoic Dongxiang-Shexian ductile shear zone (Jiangnan region, South China), *Tectonophysics,* **267,** 291–302.

Shu, L.S., Faure, M., Yu, J.H. & Jahn, B.M., 2011. Geochronological and geochemical features of the Cathaysia Block (South China): new evidence for the Neoproterozoic breakup of Rodinia, *Precambrian Res.,* **187,** 263–276.

Shu, L.S., Yu, J.H. & Wang, D.Z., 2000. Late Mesozoic granitic magmatism and metamorphism-ductile deformation in the Changle-Nanao fault zone, Fujian Province, *Geol. J. China Univ.,* **6,** 368–378.

Shu, L.S., Zhou, G.Q., Shi, Y.S. & Yin, J., 1994. Study of the high pressure metamorphic blueschist and its Late Proterozoic age in the Eastern Jiangnan belt, *Chin. Sci. Bull.,* **39,** 1200–1204.

Shu, L.S., Zhou, X.M., Deng, P., Wang, B., Jiang, S.Y., Yu, J.H. & Zhao, X.X., 2009. Mesozoic tectonic evolution of the Southeast China Block: new insights from basin analysis, *J. Asian Earth Sci.,* **34,** 376–391.

Si, J. & Van der Voo, R., 2001. Too-low magnetic inclinations in central Asia: an indication of a long-term Tertiary non-dipole field? *Terra Nova,* **13,** 471–478.

Sun, Z., Yang, Z., Yang, T., Pei, J. & Yu, Q., 2006. New Late Cretaceous and Paleogene paleomagnetic results from South China and their geodynamic implications, *J. geophys. Res.,* **B111,** doi:10.1029/2004JB0034555.

Tamai, M., Liu, Y.Y., Lu, L.Z., Yokoyama, M., Halim, N., Zaman, H. & Otofuji, Y., 2004. Palaeomagnetic evidence for southward displacement of the Chuan Dian Fragment of the Yangtze block, *Geophys. J. Int.,* **158,** 297–309.

Tan, X., Gilder, S., Kodama, K., Jian, W., Han, Y., Zhang, H.M., Xu, H. & Zhou, D., 2010. New paleomagnetic results from the Lhasa block: revised estimation of latitudinal shortening across Tibet and implications for dating the India-Asia collision, *Earth planet. Sci. Lett.,* **293,** 396–404.

Tan, X., Kodama, K., Chen, H., Fang, D., Sun, D. & Li, Y., 2003. Paleomagnetism and magnetic anisotropy of Cretaceous redbeds from the Tarim basin, northwest China: evidence for a rock magnetic cause of anomalously shallow paleomagnetic inclinations from central Asia, *J. geophys. Res.,* **108B,** doi:10.1029/2001JB001608.

Tapponnier, P., Peltzer, G., Le Dain, A.Y., Armijo, R. & Cobbold, P., 1982. Propagating extrusion tectonics in Asia: new insights from simple experiments with plasticine, *Geology,* **10,** 611–616.

Tauxe, L. & Kent, D.V., 1984. Properties of a detrital remanence carried by hematite from study of modern river deposits and laboratory redeposition experiments, *Geophys. J. R. astr. Soc.,* **77,** 543–561.

Torsvik, T.H. & Van der Voo, R., 2002. Defining Gondwana and Pangea palaeogeography: estimates of Phanerozoic non-dipole (octupole) fields, *Geophys. J. Int.,* **151,** 771–794.

Tsuneki, Y., Morinaga, H. & Liu, Y., 2009. New palaeomagnetic data supporting the extent of the stable body of the South China Block since the Cretaceous and some implication on magnetization acquisition of redbeds, *Geophys. J. Int.,* **178,** 1327–1336.

van der Voo, R., 1990. The reliability of paleomagnetic data, *Tectonophysics,* **184,** 1–9.

van der Voo, R. & Torsvik, T.H., 2001. Evidence for late Paleozoic and Mesozoic non-dipole fields provides an explanation for the Pangea reconstruction problems, *Earth planet. Sci. Lett.,* **187,** 71–81.

Wang, F. *et al.*, 2010. The boundary ages of the late Mesozoic volcanic-sedimentary strata on South China: Constrains from 40Ar/39Ar geochronology and paleomagnetism (in Chinese), *Sci Sin Terra,* **40,** 1552–1570.

Wang, Y., Yu, D.J., Guan, T.Y., Liu, P.H. & Wu, J.H., 2002a. Petrological and petrochemical characteristics of Early Cretaceous volcanic rocks in northeast Jiangxi Province, *Acta Petrol. Mineral.,* **21,** 31–48 (in Chinese with English abstract).

Wang, Y., Guan, T.Y., Huang, G.F., Yu, D.J. & Chen, C.L., 2002b. Isotope chronological studies of Late Yanshanian volcanic rocks in Northeast Jiangxi Province, *Acta Petrol. Mineral.,* **23,** 233–236 (in Chinese with English abstract).

Wang, B. & Yang, Z., 2007. Late Cretaceous paleomagnetic results from southeastern China, and their geological implication, *Earth planet. Sci. Lett.,* **258,** 315–333.

Wang, D.Z. & Shu, L.S., 2012. Late Mesozoic basin and range tectonics and related magmatism in Southeast China, *Geosci. Front.,* **3,** 109–124.

Wang, X.L., Zhou, J.C. & Griffin, W.L., 2007. Detrital zircon geochronology of Precambrian basement sequences in the Jiangnan orogen: dating the assembly of the Yangtze and Cathaysia Blocks, *Precambrian Res.,* **159,** 117–131.

Watson, G.S., 1956. A test for randomness of directions, *Mon. Not. R. astr. Soc. Geophys. Suppl.,* **7,** 160–161.

Xu, J., Zhu, G., Tong, W.X., Gui, K.R. & Liu, Q., 1987. Formation and evolution of the Tancheng-Lujiang wrench fault system: a major shear system to the northwest of the Pacific Ocean, *Tectonophysics,* **134,** 273–310.

Yang, Z. & Besse, J., 2001. New Mesozoic apparent polar wander path for south China: tectonic consequences, *J. geophys. Res.,* **106,** 8493–8520.

Yoshioka, S., Liu, Y.Y., Sato, K., Inokuchi, H., Su, L., Zaman, H. & Otofuji, Y., 2003. Paleomagnetic evidence for post-Cretaceous internal deformation of the Chuan Dian Fragment in the Yangtze block: a consequence of indentation of India into Asia, *Tectonophysics,* **376,** 61–74.

Yu, Y.W., Xu, B.T., Chen, J.F. & Dong, C.W., 2001. Nd isotopic systematics of the Late Mesozoic volcanic rocks from southeastern Zhejiang Province, China: implications for stratigraphic study, *Geol. J. China Univ.,* **7,** 62–69 (in Chinese with English abstract).

Yu, X.Q., Shu, L.S., Yan, T.Z., Zu, F.P. & Wang, B., 2004. Geochemistry of basalts of late period of Early Cretaceous from Jiangshan-Guangfeng, SE China and its tectonic significance, *Geochemica,* **33,** 465–476 (in Chinese with English abstract).

Zhao, X. & Coe, R.S., 1987. Palaeomagnetic constraints on the collision and rotation of North and South China, *Nature,* **327,** 141–144.

Zhou, X.M., Sun, T., Shen, W.Z., Shu, L.S. & Niu, Y.L., 2006. Petrogenesis of Mesozoic granitoids and volcanic rocks in South China: a response to tectonic evolution, *Episodes,* **29,** 26–33.

Zhu, Z., Hao, T. & Zhao, H., 1988. Paleomagnetic study on the tectonic evolution of Pan-Xi block and adjacent area during Yinzhi-Yanshan period, *Acta geophys. Sin.,* **31,** 420–431.

Zhu, Z., Morinaga, H., Gui, R., Xu, S. & Liu, Y., 2006. Paleomagnetic constraints on the extent of the stable body of the South China block since the Cretaceous: new data from the Yuanma Basin, China, *Earth planet. Sci. Lett.,* **248,** 533–544.

Zijderveld, J.D.A., 1967. A. C. demagnetization of rocks: analysis of results, in *Methods in Palaeomagnetism,* pp. 254–286, eds Collinson, D.W., Creer, K.M. & Runcorn, S.K., Elsevier, Amsterdam.

Zonenshain, L.P., Kuzmin, M.I. & Moralev, V.M., 1990. *Geology of the USSR: a plate tectonic synthesis,* Geodynamics Series, Vol. 21, pp. 242, AGU, Washington, DC.

Zorin, Y.A., 1999. Geodynamics of the western part of the Mongolia–Okhotsk collisional belt, Trans-Baikal region (Russia) and Mongolia, *Tectonophysics,* **306,** 33–56.